# MAXIMUM POWER POINT TRACKING OF HYBRID SYSTEM USING INCREMENTAL CONDUCTANCE METHOD

A Dissertation submitted in fulfilment of the requirements for the Degree

of

**MASTER OF ENGINEERING**

*in*

**Power Systems**

*Submitted by*

Rupali Singh
801742019

*Under the Guidance of*

Dr. Amrita Sinha
Assistant Professor, EIED

Dr. Parag Nijhawan
Associate Professor, EIED

THAPAR INSTITUTE
OF ENGINEERING & TECHNOLOGY
(Deemed to be University)

**2019**

**Electrical and Instrumentation Engineering Department**

**Thapar Institute of Engineering & Technology, Patiala**

***(Declared as Deemed-to-be-University u/s 3 of the UGC Act., 1956)***

**Post Bag No. 32, Patiala – 147004**

**Punjab (India)**

# DECLARATION

Certified that the dissertation entitled, "Maximum Power Point Tracking of Hybrid System using Incremental Conductance Method", which is being submitted by Rupali Singh in fulfillment of the requirements for the award of the M.E. Power Systems, to Thapar Institute of Engineering & Technology (Deemed to be University), is a bona-fide record of the candidate's own work carried out by her under my supervision and guidance. The matter contained in this dissertation has not been submitted, neither in part nor in full to any other university or institute for award of any degree.

Rupali.

Place: Patiala
Date: 18-09-2019

**Rupali Singh**
**Roll No.: 801742019**

It is certified that the above statement made by the student is correct to the best of my knowledge and belief.

18/9/19

**(Dr. Amrita Sinha)**
Assistant Professor, EIED

Parag 18/09/19

**(Dr. Parag Nijhawan)**
Associate Professor, EIED



i

# ACKNOWLEDGEMENT

With great pleasure and privilege, I wish like to express my grateful sense of gratitude and indebtedness to Dr. Amrita Sinha (Assistant Professor) and Dr. Parag Nijhawan (Associate Professor), EIED, TIET, Patiala for her patient guidance and support throughout this dissertation. I found her guidance valuable and more importantly her supportive and motivating approach.

I am also thankful to Dr. R. S. Kaler, Professor & Head, EIED for his assistance and support. I am also thankful to faculty of EIED for extending their cooperation. I wish to thank my friends who devoted their valuable time and helped me in all possible ways towards successful completion of this dissertation. I thank all those who have contributed directly or indirectly to this dissertation.

Lastly, I would like to thank my parents for their years of unyielding love and encouragement. They have always wanted the best for me and admire their determination and sacrifice.

**Rupali Singh**

(801742019)

# TABLE OF CONTENTS

# LIST OF TABLES

# LIST OF FIGURES

# LIST OF ABBREVATIONS

| | |
|---|---|
| PV | Photo voltaic |
| MPPT | Maximum Power Point Tracking |
| P&O | Perturb and observe |
| IC | Incremental Conductance |
| PMSG | Permanent magnet synchronous generator |
| DFIG | Doubly fed induction generator |
| MPP | Maximum power point |
| BESS | Battery energy storage system |
| PWM | Pulse width modulation |

# NOMENCLATURE

| | |
|---|---|
| $I_{PV}$ | Photocurrent |
| $I_0$ | Reverse saturation current of diode |
| $V$ | Voltage across the diode |
| $a$ | Ideality factor |
| $V_T$ | Thermal voltage |
| $R_S$ | Series resistance |
| $R_P$ | Shunt resistor of the cell |
| $K_I$ | Cell's short circuit current temperature coefficient |
| $G$ | Solar irradiation in W/m$^2$ |
| $G_{STC}$ | Nominal solar irradiation in W/m$^2$ |
| $I_{PV\_STC}$ | Light generated current under standard test condition |
| $I_{0\_STC}$ | Nominal saturation current |
| $E_g$ | Energy band gap of semiconductor |
| $T_{STC}$ | Temperature at standard test condition |
| $q$ | Charge of electrons |
| $I_{SC\_STC}$ | Short circuit current at standard test condition |
| $V_{OC\_STC}$ | Short circuit voltage at standard test condition |
| $K_V$ | Temperature coefficient of open circuit voltage |
| $N_S$ | Number of series cells |
| $N_P$ | Number of parallel cells |
| $P_M$ | Power captured by wind turbine |
| $\rho$ | Air density |
| $\beta$ | Pitch angle (in degree) |
| $R$ | Blade radius (in meters) |
| $V$ | Wind speed (in m/s) |
| $p$ | The number of pole pair in the generator |
| $V_{ph}$ | Generator output |
| $f$ | Frequency of rotor |

| | |
|---|---|
| $\varphi$ | Flux |
| $t$ | Number of turns |
| $V_O$ | Output of Buck-boost converter |
| $V_w$ | Input of buck-boost converter |
| $P$ | Wind rotor |
| $\Omega$ | Rotor speed |
| $\Omega_e$ | Generator- phase voltage angular speed |
| $V_W$ | Rectifier output voltage |
| $D$ | Duty cycle of converter |
| $C_p$ | Wind turbine power coefficient |
| $\lambda$ | Tip-speed ratio |
| $\lambda_1$ | Constant |
| $\Omega$ | Rotor speed of rotation (in rad/sec) |

# ABSTRACT

Renewable energy sources have become a popular alternative energy source where conventional power generation techniques are inconvenient. Over the past few years, the generation of photovoltaic and wind power has increased significantly. In this study, we proposed a hybrid energy system incorporating solar panels and wind turbine generators as an alternative to conventional electrical systems. A straightforward, cost-effective control technique was suggested to monitor the point where maximum energy can be coerced under constantly changing environmental conditions from the PV and wind turbine generator system. In combination with comprehensive simulation results, the entire hybrid system is described to uncover the feasibility of the scheme.

This dissertation concerned to presents a control and simulation of hybrid renewable energy system connected to the grid. The studied system includes a photovoltaic panel, doubly fed induction generator based wind turbine, and a battery for storage energy. The PV array and wind systems are connected to the common DC bus by a boost converter. The battery is connected by a bi-directional DC/DC converter, and then integrated into the AC utility grid via a common DC/AC inverter. To extract the maximum energy, a simulation study has been carried out according to the meteorological conditions (wind speed and variable solar irradiance) while maintaining power quality at a satisfactory level. To capture the maximum power, a MPPT algorithm is applied for both wind turbine and photovoltaic panel.

# CHAPTER-1
# INTRODUCTION

## 1.1 Overview

In present scenario, renewable energy sources are fused along with battery energy storage systems, which mostly used for the maintenance of the power reliability. The most of the renewable energy sources increased as the distribution sources, generally for the improvement of the power supply stability and hence power quality with the new policies of operations are essential. The common drawback of the wind and solar power plants are unreliable power.

In order to overwhelmed this problem an innovative practice is implemented i.e. maximum power point tracking algorithm which is appropriate to wind and solar system. Dynamic concert of wind and solar system has analysed. There are the some previous work on hybrid systems including of wind energy, photovoltaic and battery has been discussed. Entire energy sources has modelled using MATLAB tool to analyse the behaviour.

A simple control on the method trails the maximum power from the wind and PV energy source to achieve abundant higher engendering capacity factor. The simulation result prove viability and dependability of this system.

In current years, the renewable energy systems is used to produce the electrical energy that transferred by electric network on more or less distance to the manipulators. Till nowadays, these individual systems that deliver electricity to the small groups are extensive. They are suitable in sites where public network linking is problematic. In case where there is two types of connection of the wind systems , then a first system which is linked to the grid and the second called self-regulating used in places where it would not be connected to grid.

Fig. 1.1 show the block diagram of hybrid system.

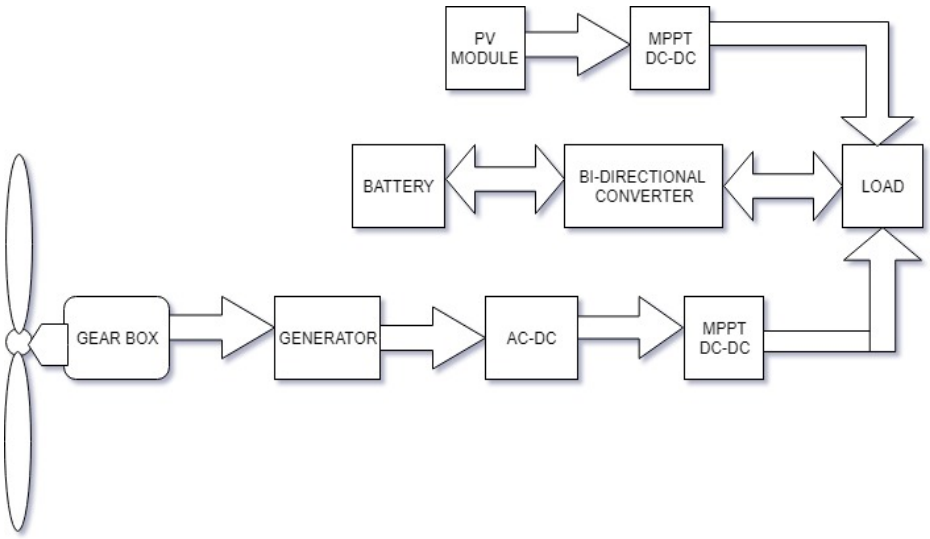


Fig 1.1. Block diagram of hybrid system

Wind turbine, generator, gear box, and the AC – DC converter included in wind energy system. The wind turbine which is used to convert the wind energy to the rotational mechanical energy and this rotational mechanical energy available at shaft is transformed to electrical energy using the generator. To coerce maximum power from the wind system we used the maximum power point tracing system.

The contribution of this work is to study the multi-source system based on wind, photovoltaic (PV) panels and batteries in order to inject the energy produced in an island or rural electric network.

### 1.2 Literature Review

S. Rahman *et al.* [1] presented the linear programming methods to minimalize the average production cost of electricity while conference the load requirement in a consistent manner and take the environmental factor into the consideration of both in the design and operation points and gives the concept of optimal design of hybrid (wind-PV) system for whichever autonomous or grid linked applications.

T. Markvart *et al.* [2] discussed the procedure for regulates the sizes of the PV array and wind turbine in a (PV-wind) hybrid system. Using the restrained data of PV and wind at a given site, Markvart employ the simple graphical structure to determine optimum formation of two generators that placates the energy demand of handler throughout the year.

K. Katti and M. K. Khedkar *et al.* [3] developed the algorithm practices hourly average insolation, wind speed, and the power demand to regulate (Wind-PV) generation measurements required to encounter demand deprived of the loss of power supply prospect.

S.M. Shaahid *et al.* [4] developed the optimum battery storage size for the hybrid wind energy system by reviewing an influence of variation of the battery storage capacity on the hybrid power generation and anticipated the opportunities for consumption of stand-alone hybrid (PV-battery) power system in hot climates. Trade-off among size of the diesel power and storage capacity essential for the load presumptuous the constant wind power output was also reported by Shaahid.

E. Koutroulis *et al.* [5] offered a practice for the optimal sizing of stand-alone (PV-wind) system with genetic algorithm. They pragmatic the design approach for the power generation system which provisions a inhabited household. Optimum size of hybrid (PV-wind) energy system can be considered on an hourly basis or on the basis of day-to-day average power per month the day of least PV power per month, and the day of least wind power per month. Performance of hybrid (PV-wind) energy system has compared on the hourly basis, by fixing capacity of the wind generators, yearly loss of load prospect with different capacity of PV array and battery bank are premeditated.

A.H. Shahirinial *et al.* [6] related the results of two optimization procedures based on simplex and different algorithm for hybrid (PV-wind) system. He offered the method for valuation on the basis of loss of load prospect to decide the optimal proportion of (PV-wind) generator capacities in hybrid PV-wind system, optimal system amalgamation has selected on the basis of the capital cost and annual self-sufficiency level. Self-sufficiency level of a system is defined in terms of the loss of load prospect and is been used to find the system conformation.

C. Protogeropoulos *et al.* [7] established the general procedure by considering the design factor such as self-sufficiency, for sizing and optimization and presented the complete set of calculation methods for the optimum sizing of (PV-wind) hybrid system. In this method, the more accurate and the practical mathematical model for characterizing PV module, wind generator and battery has adopted, combining with the hourly measured climatological data and load data, the concert of a (PV-wind) hybrid system is resolute on hourly basis, by fixing capacity of the wind generators, the whole year's loss of power source probability values of (PV-wind) hybrid systems with the different capacity of PV arrangement and battery set has been calculated, then a trade-off curve between the battery set and PV array measurements is drawn for a given loss of the power supply probability worth, the optimum conformation which can meet energy demand with a minimum cost can be initiate by drawing a tangent to the trade-off curve with slope representing affiliation between cost of PV module and that of the battery set.

H. Yang *et al.* [8] established the novel optimization sizing model for the hybrid (PV-wind) power cohort system. To optimize the capacity sizes of the different apparatuses of the hybrid (PV-wind) power generation systems commissioning a battery set, Yang likewise calculated the battery size necessities to achieve the desired level of the self-sufficiency by using the system concert simulation model. From this it has been observed that for attaining high autonomy, a backup generator is needed and in turn condenses battery storage capacity and also conferred the method to optimize hybrid (PV-wind and battery) system with conservative power plant and designed optimal system arrangement on foundation of life cycle cost.

M. D. Arifujjaman *et al.* [9] offered the lively modelling of minor wind turbine with tie up subtleties. Also these small wind turbines based on the permanent magnet generator and their speed can be controlled by implementing the load control. The abstraction of the maximum power output from these wind turbines are examined using tip-speed ratio control and the hill-climbing control approaches. The system is simulated in MATLAB/ Simulink to determine the suitable control approach.

B.S. Borowy *et al.* [10] deliberated the lively response of stand-alone wind energy adaptation system with battery energy storage system to the wind gust. Borowy anticipated the mathematical model for each element of a standalone wind energy system. This model variables are articulated in the (d -q) rotor reference frame. The wind turbine has been considered as the only basis of power in this research. Using this model the system rejoinder to recorded wind gust is examined by manipulative generator current, load current, battery charging current, rectifier current and battery voltage.

V.R. Pawar *et al.* [11] presented the energy mandate is ever cumulative in the world, searching for fossil fuel is done on precedence basis. These fuels are not maintainable, they pollute environment. Deficiency of fossil fuels resources and contrary environment distresses has made use of the renewable energy sources as Solar energy and Wind energy indispensable. Solar energy and Wind energy are accepted resources which are not exhausted by the use and are more prevalent. Obtainability and ease to obtain the electric power made the Solar and Wind power as substitute energy sources. Solar energy and Wind energy collective to form the (PV-wind) Hybrid Power System, which will augment the abilities of each other and alternative. Constant voltage method is adopted for the maximum power transfer of (PV-wind) hybrid system. This method has been experienced the topographies to increase the constancy and effectiveness.

### 1.3 Objectives of Work

The foremost objective of the work is to contrivance a power system that is a hybrid of composed Photovoltaic and the wind powers. The formulation of the purposes are given in following steps:

- Modelling of maximum power point tracking of photovoltaic system.
- Modelling of maximum power point tracking system of wind energy system.
- Modelling of the hybrid system of photovoltaic, wind and battery energy storage system using the incremental conductance method.

### 1.4 Organisation of the Dissertation

Presented work is alienated into six chapters.

Chapter 1 contains introduction to Hybrid energy system of photovoltaic, wind and battery energy storing system and algorithm use to implemented in the system. It also review over the different types of limiters and their applications in the renewable system.

Chapter 2 covers the brief description of photovoltaic energy system and MPPT of PV module.

Chapter 3 covers the brief description of wind energy system and MPPT of wind energy system.

Chapter 4 includes battery energy storage system and their applications.

Chapter 5 contains the incremental conductance MPPT techniques in hybrid system.

Chapter 6 has result and discussion of the hybrid system using the incremental conductance MPPT.

Chapter 7 is conclusion of work along with future scope.

# CHAPTER-2
# PHOTOVOLTAIC SYSTEM

## 2.1 Photovoltaic arrangement

A photovoltaic energy system is primarily power-driven by solar energy. The conformation of PV system established in figure 2.1.

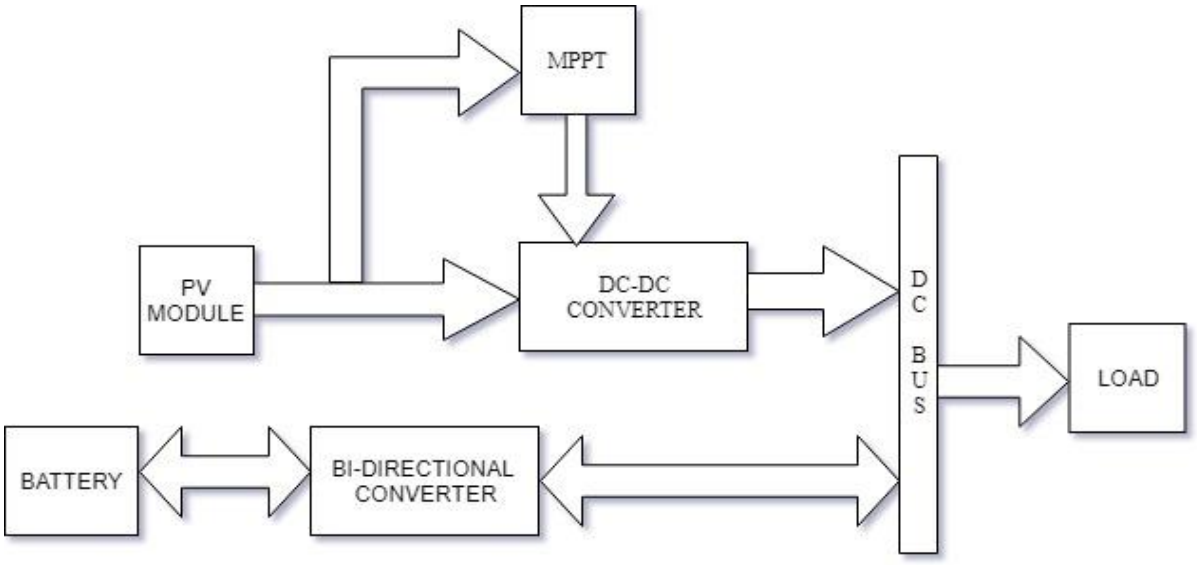


Fig. 2.1. Overall block diagram of the PV system

It comprises photovoltaic modules or arrays which adapt the solar energy in form of solar irradiation into the electric energy. DC-DC converter vicissitudes the level of voltage to contest it with electrical appliances which are supplied by the system. This DC-DC converter may be either buck or boost or buck-boost depending on the requirement and obtainable voltage levels. The maximum power point tracking system forces the maximum power from PV modules. The bi-directional converter is able to source the current in both the orders is used to charge battery when there is surplus power and that of energy stored by battery has discharged across load when there is a deficiency of power.

### 2.1.1 PV cell

Photovoltaic cell is a building block of PV system and the semiconductor material such as the silicon and germanium are building block of the PV cell. Silicon is adapt for photovoltaic cell due to the benefit over the germanium. When photons stikes the surface of the solar cell, the electrons and holes generated by contravention the covalent bond inside the atom of the semiconductor material and in retort electric field has generated by generating positive and negative terminals. When the terminals are connected by conductor current will start flowing through the cell. This current is used to produce the power across the load. Structure of the PV cell manifested in fig. 2.2.

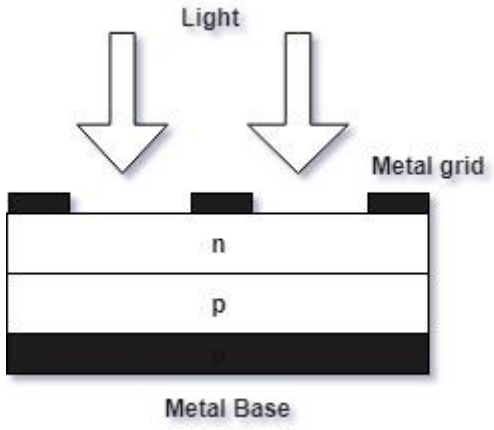


Fig. 2.2. PV cell

### 2.1.2 PV module

Generally a single cell produces a very low voltage approximately about 0.4 volts so that more than one PV cells can be associated moreover in serial or in parallel or grid as the both serial and parallel, to arrangement of PV module as shown in fig.2.2. When the requirement is of higher voltage, we join PV cell either in series and if the demand of load is high current then connect PV cell as in parallel. As in particular, there are 36 or 76 cells in generally PV modules. The front side of module is transparent other than build-up of low-iron and transparent glass material and the PV cell is summarized. The effectiveness of a module is not virtuous as PV cell due to the reason of glass cover and frame reflects in some expanse of inward radiation.

### 2.1.3 PV array

Photovoltaic array simply is the interconnection of the several PV modules in serial or in parallel. The power produced by the individual modules may not moreover be sufficient to meet the need of transaction applications, so that the modules are available in grid form or as an array to satisfy load demand. In PV array modules are associated like as that of cells connected in module. However making a PV array usually modules are originally connected in a series way to obtain anticipated voltage, and then the strings as attained are connected in parallel in conclusion to produce the additional current based on the need.

## 2.2 Working of a PV cell

The elementary concept involved in working of the specific PV cell is the Photoelectric effect conferring to that when photon particle strikes PV cell, subsequently receiving energy from the sunbeam electrons from the semiconductor gets excited and stage to the conduction band from valence band and turn out to be free to move. Moreover movement of the electrons produce positive and negative terminal and consequently create the potential difference across those two terminals. When external circuit is associated between these two terminals, electric current starts flowing through the circuitry. Fig. 2.3 shows the concept of PV cell.

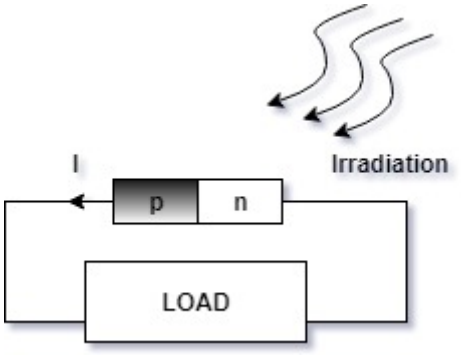


Fig. 2.3. Working of a PV cell [9]

## 2.3 Modelling of a PV cell

Usually photovoltaic system changes sunlight directly to electrical energy without having any calamitous effect on the environment. The basic section of the PV array is PV cell which has in particular a modest p-n junction device. The fig.2.3 establishes the equivalent circuit of a PV cell [12]. Equivalent circuit carries the current source as photocurrent and diode which is parallel to that resistor is in series relating an internal resistance to flow of current and that of

shunt resistance which implies the leakage current. The current provided to load can be stated as in equation (2.1)

$$\boldsymbol{I} = \boldsymbol{I_{PV}} - \boldsymbol{I_0}\left[\exp\left(\frac{V+IR_S}{aV_T}\right) - 1\right] - \left(\frac{V+IR_S}{R_P}\right) \quad (2.1)$$

Where,

$I_{PV}$– Photocurrent current

$I_O$ – Diode Reverse saturation current

$V$– Voltage across diode

$a$ – Ideality factor

$V_T$ –Thermal voltage

$R_S$ – Series resistance

$R_P$ – Shunt resistance

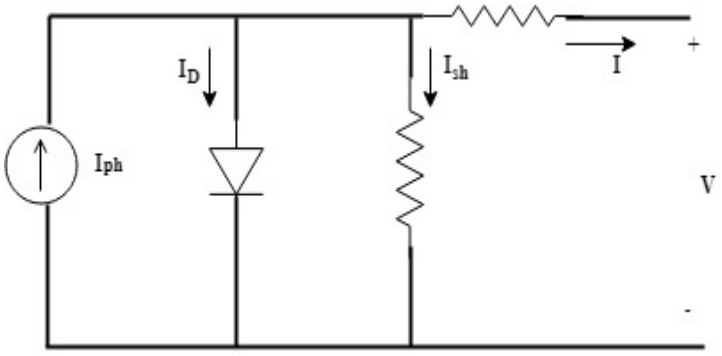


Fig. 2.4. Equivalent circuit of the diode of solar cell

Fig. 2.4. is the equivalent circuit of diode modal of the solar cell. The photovoltaic cell photo current which be subject to the radiation and the temperature can be stated as equation (2.2)

$$I_{PV} = (I_{PV-STC} + K_I \Delta T)\frac{G}{G_{STC}} \quad (2.2)$$

Where,

$K_I$ - cell short circuit current temperature coefficient

$G$ - solar irradiation (W/m$^{2)}$

$G_{STC}$ - nominal solar irradiation (W/m$^{2)}$

$I_{PV\_STC}$ -light generated current under the standard test condition

The reverse saturation current differs as a cubic function of the temperature which stated as in equation (2.3)

$$I_0 = I_{0_{STC}} \left(\frac{T_{STC}}{T}\right)^3 \exp\left[\frac{qE_g}{aK}\left(\frac{1}{T_{STC}} - \frac{1}{T}\right)\right] \quad (2.3)$$

where,

$I_{0\_STC}$ - minimal saturation current

$E_g$ - energy band gap of the semiconductor

$T_{STC}$ - temperature at the standard test condition

$q$ - charge of the electron

The reverse saturation current is moreover improved as purpose of the temperature as given in equation (2.4)

$$I_0 = \frac{(I_{SC_{STC}} + K_I \Delta T)}{\exp\left[\frac{(V_{OC_{STC}} + K_V \Delta T)}{aV_T}\right] - 1} \quad (2.4)$$

Where,

$I_{SC\_STC}$ – short circuit current for standard test condition

$V_{OC\_STC}$ – open circuit voltage for standard test condition

$K_V$ – temperature coefficient for open circuit voltage

For greater precision and for distinct reasons, many writers suggested more advanced models. In some models, an additional diode represents the impact of carrier recombination. Some writers also used three models of diodes that included factors from some other impacts not well thought-out in earlier representations. But usually the use of single diode prototypical for work for the reason that of ease.

The effectiveness of PV cell does not be subject to the dissimilarity in the cell's shunt resistance Rp, but effectiveness of a PV cell be subject to the heavily on variation in the Rs series resistance. Since the cell's Rp is contrarywise proportional to ground shunt leakage current so that it can expected to be very high for a minor leakage to the ground.

Due to incidentally minor full energy produced by only PV cell one can used mixture of the PV cells to meet the required demand. In particular to that PV cell grid is identified as the PV arrays. PV array equations can depicted as equation (2.5)

$$I = I_{PV}\, N_P - I_O N_P \left[exp\left(\frac{V + IR_S\left(\frac{N_S}{N_P}\right)}{aV_T N_S}\right) - 1\right] - \left(\frac{V + IR_S\left(\frac{N_S}{N_P}\right)}{R_P\left(\frac{N_S}{N_P}\right)}\right) \quad (2.5)$$

Where,

$N_S$ – Number of the series cell

$N_P$ – Number of the parallel cell

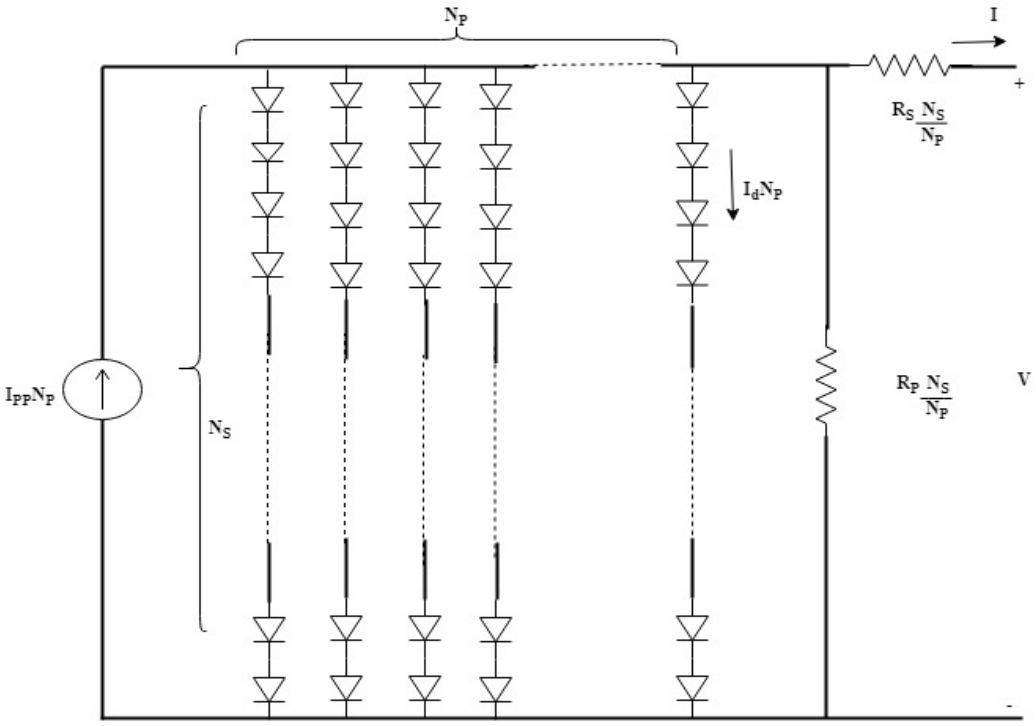


Fig. 2.5. Representation of PV module

Fig. 2.5. manifested representation the minor modification in the series resistance may have a greater impact on a PV cell's effectiveness, but shunt resistance variation does not have a greater impact. Usually the shunt resistance is presumed as an infinite and handled as the open for very tiny leakage present to ground. The model's mathematical equation be articulated as later in view of shunt resistance endlessness and given as in equation (2.6)

$$I = I_{PV}\, N_P - I_O N_P \left[ exp\left( \frac{V + IR_S\left(\frac{N_S}{N_P}\right)}{aV_T N_S} \right) - 1 \right] \tag{2.6}$$

PV module characteristics of the I-V and P-V are shown in fig 2.6 and 2.7 correspondingly.

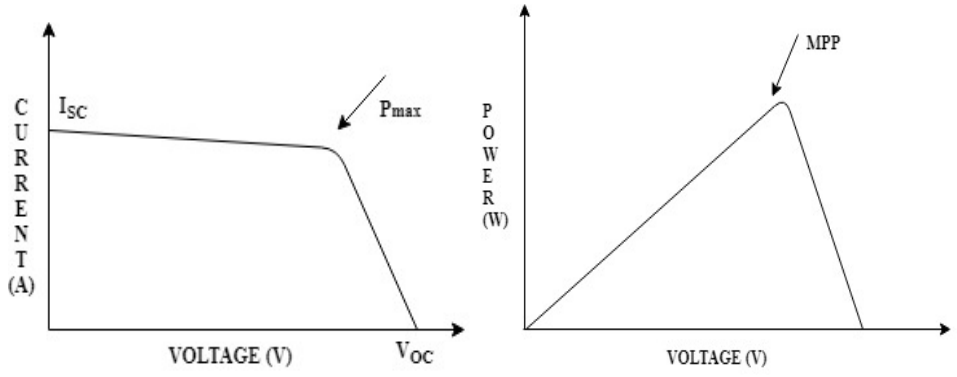


Fig. 2.6. I-V characteristics

Fig. 2.7. P-V characteristics

Two parameters which are incorporated to relate electrical concert are open-circuit voltage of cell ($V_{oc}$) and the short-circuit current of cell ($I_{sc}$).

The maximum power given as in equation (2.7)

$$P_{max} = V_{max}\, I_{max} \tag{2.7}$$

The parameters used for the modelling of PV module are shown in table 2.1 [13]

| SI. No. | Parameters | Value |
|---|---|---|
| 1 | $I_{mp}$ | 7.62 A |
| 2 | $V_{mp}$ | 26.4 V |
| 3 | $I_{sc}$ | 8.20 A |
| 4 | $P_{max}$ | 200.144 W |
| 5 | $V_{oc}$ | 32.8 V |
| 6 | $K_v$ | -0.1230 V/K |
| 7 | $K_t$ | 0.0032 A/K |
| 8 | $N_s$ | 54 |
| 9 | $N_p$ | 4 |

Table 2.1. PV array at $25^0$C & 1000 W/$m^2$ parameters

## 2.4. Shading Effect of PV Module

In particular, module or in part of it shaded, starts creating a lesser amount of voltage or current as compared to the unshaded one. When the modules are connected in a series alike current will drift in the entire circuitry other than the shaded portion cannot be able to produce identical current however it allows the identical current to flow through the circuitry, in conclusion to shaded portion jerks performing like load and flinches overwhelming the power. When the shaded portion starts to turn as load that condition is identified as hot-spot problematic. Generally, without suitable protection problem of the hot-spot may rise and in several situations the system might be get spoiled [15]. To diminish the impairment in this state one can usually use a bypass diode [16,17]. Block diagram of a PV array in the shaded condition is made known in below fig. 2.8.

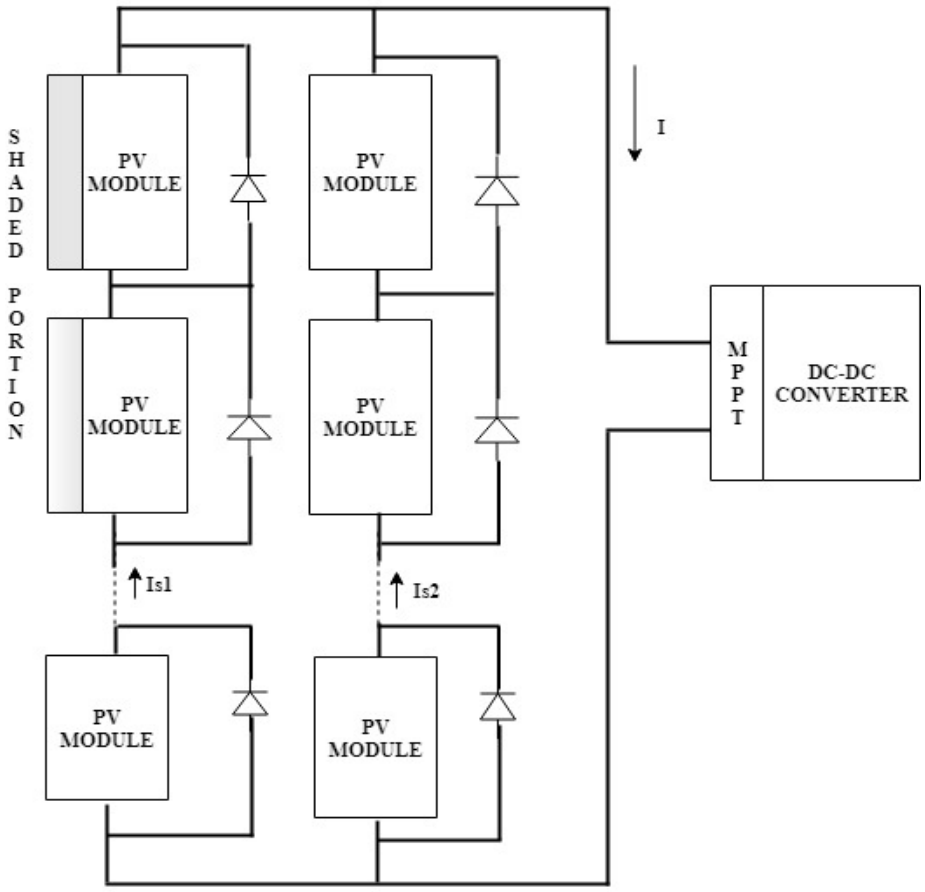


Fig. 2.8. PV Array with a shaded condition

However, due to the partial shading or entire shading PV characteristics turn out to be more non-linear and having the superfluous maximum power point [18]. So that for the condition for

this tracking of a maximum power point become identical monotonous. From the figure 2.9., it has been cleared the effect of shading of PV characteristics in the fig shown below.

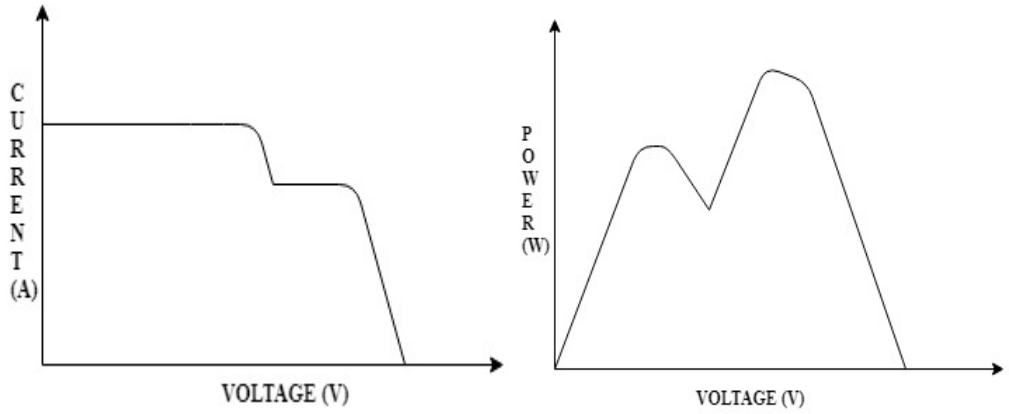


Fig. 2.9. Effect of the partial shading of I-V and P-V characteristics.

### 2.5 Maximum Power Point tracking of PV system

Maximum power point tracking (MPPT) system is the electronic control system which can be able to force the maximum power flow from PV model. Usually it does not indulge a single mechanical module that results in a movement of the components changing their directions and make them face conservative towards sun. The MPPT control system is totally electronic system which can distribute maximum permissible power by changing the operating point of the modules efficiently [19].

#### 2.5.1 Necessity of the Maximum Power Point tracking for PV system

In particular, power vs voltage distinguishing of a PV module shown in fig 2.7 it would be concluded that there exist solitary maxima that is maximum power point related to a specific voltage and current which are being supplied. The overall effectiveness of a module is very less around 12%. So in conclusion, that would be essential to function it at the crest power point so that maximum power can be provided to a load, regardless of unceasingly changing environmental circumstances. That increased power makes it restored for the use of a PV module. Also, DC-DC converter which has located next to the PV module extracts maximum power by identical the impedance of circuit to the impedance of PV module and it transfers to load. Impedance matching can be carried out by changing the duty cycle of a switching elements [20].

# CHAPTER 3

# WIND POWER SYSTEM

## 3.1 Introduction to Wind Power System

Wind power has decreased assembly expenses associated to solar power. The major problem with the wind power system is sporadically accessible which should be therefore supported by other power possessions. The wind power system excerpts and transforms wind power into electrical energy [22]. The wind power system power differs depending on a wind speed. Due nonlinear characteristic of a wind turbine, this has stimulating duty to continue the maximum power output of wind turbine for all the wind speed situations. In particular, wind speed differs unpredictably, the model for simulating wind energy system is easy to develop.

## 3.2 System Configuration

The wind energy system's schematic illustration is shown in figure below fig. 3.1.

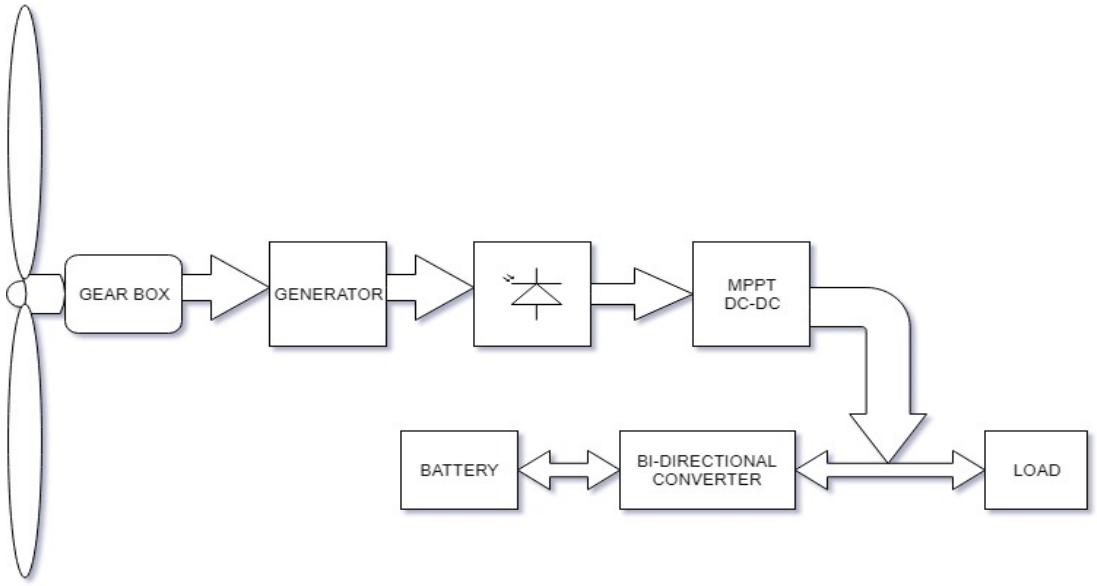


Fig. 3.1. Block Diagram of the wind power system

The system consists of a wind turbine that alters wind kinetic energy into a rotating movement and the gearbox that matches the turbine velocity to a generator velocity, a generator that alters mechanical energy into the electrical energy, rectifier that converts ac voltage to dc voltage also dc-dc converter that can be precise to trace the maximum power point the battery would be charge and discharge through the bi-directional converter.

### 3.3 Wind Turbine Generator

Generally wind turbine comprises of a conventional rotor blades rotating about a hub and inside nacelle there is a set of gearbox generators. A figure 3.2. below given is the basic working of wind turbine system.

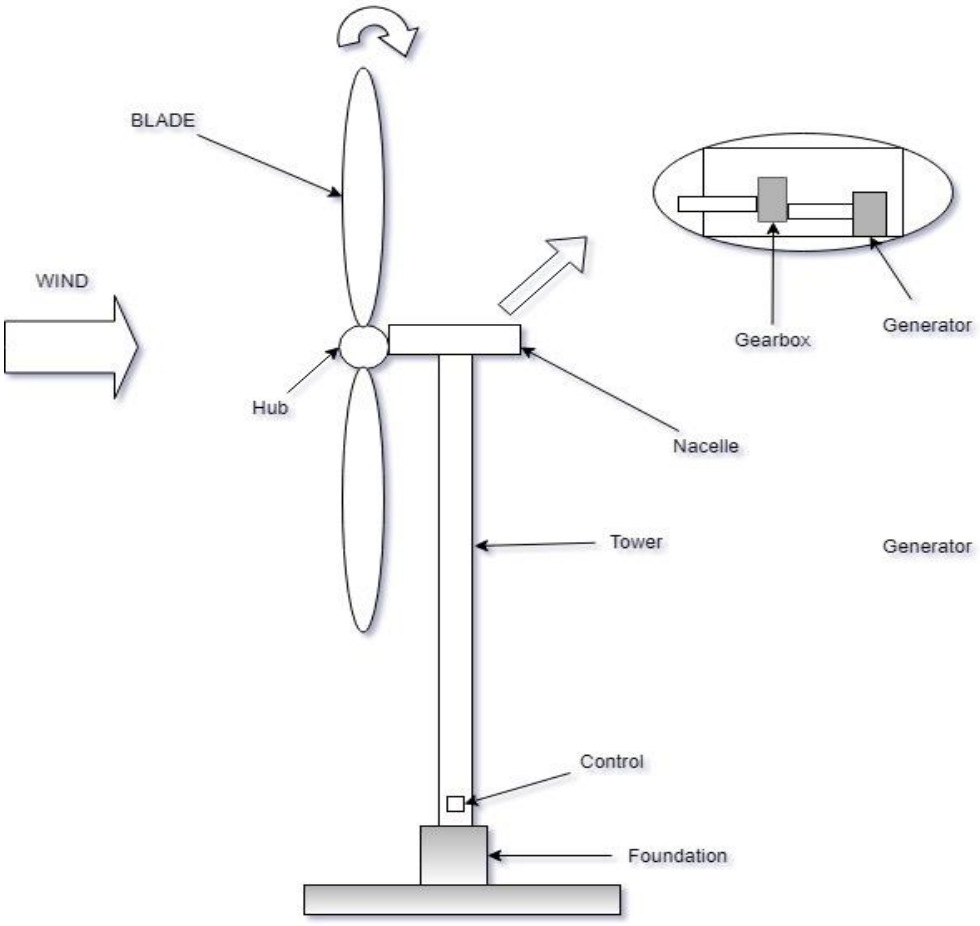


Fig. 3.2. Working of a wind turbine [23]

Based on the axes, the wind turbines are divided into two types: the wind turbine with the vertical axis and the wind turbine with the horizontal axis.

#### 3.3.1 Modelling of wind turbine

A wind turbine transforms kinetic air energy that is wind power, into mechanical power and that of turbine rotational motion which further can be used straight to operate the machine or used to operate generator. Wind turbine blade apprehended power is a affiliated of blade form, rotation velocity, pitch angle, radius of a rotor [24]. Below is the equation (3.1) for the produced energy.

$$P_M = \frac{1}{2} \pi C_\rho (\lambda,\beta) R^2 V^3 \quad (3.1)$$

where,

$P_M$ - Power captured by a wind turbine

$\rho$ - Air density factor

$\beta$ - Pitch angle measured in degrees

$V$- Wind speed measured in m/s

The term λ is known as the tip-speed ratio, stated by the equation (3.2)

$$\lambda = \frac{\Omega R}{V} \quad (3.2)$$

where,

Ω - rotor speed of the rotation measured in rad/sec

$C_p$ expressed as function of a tip-speed ratio (λ) are as shown in below equation (3.3) and (3.4),

$$C_p = \frac{1}{2}\left(\frac{116}{\lambda_1} - 0.4\,\beta - 5\right) exp^{-\frac{16.5}{\lambda_1}} \quad (3.3)$$

$$\lambda_1 = \left(\frac{1}{\frac{1}{\lambda+0.089} - \frac{0.035}{\beta^3+1}}\right) \quad (3.4)$$

Where,

$C_p$ - wind turbine power coefficient

$\lambda$ - Tip-speed ratio

$\lambda_1$ – constant function

### 3.4 Generator

Usually, wind turbine shaft is reflexively connected to the generator rotor shaft, transmitting to the rotor shaft the mechanical power formed by the wind turbine which is followed by the kinetic energy to mechanical energy conversion. Rotor winding consists of (either field or armature) in this rotor framework.

In both cases that is in stationary magnetic field, we get moving conductor or in a stationary conductor in a affecting magnetic field. In either case, the generator principle generates electrical voltage.

### 3.4.1 Classification of generator

Generators further be categorized on a present category basically. Current generators and a direct current generators are alternating. But when there is a voltage generated alternates in either case. One can be able to convert it to direct current by adding a commutator[25]. So we're going for alternating current generator for comfort.

We can further classify them in the AC generators based on the velocity of the rotor. The generators are synchronous (steady velocity machine) and asynchronous (varying velocity machine or induction machine). There is a rotor is of silent pole and a non-salient pole is of cylindrical type rotor in the synchronous generators. We can go for high-speed cylindrical rotor and low-speed rotor which is salient pole based on the speed requirement/availability.

The magnetic field is based on another classification. Either a permanent magnet or an electro-magnet can make the magnetism. Generally, permanent magnet synchronous generator (PMSG) for power generation uses the wind energy to decrease the supply requirement.

An adverse slip induction motor can be second-hand as an induction generator. Conversely generator is not of self-exciting and fixed frequency of source must excite this. That requires a stator exciter already. This machine must therefore be supplied by two supplies and consequently referred to as a double-fed induction generator.

So doubly fed induction generator (DFIG) and the permanent magnet synchronous generator (PMSG) are appropriate for the generation of wind power.

## 3.5 MPPT of a wind power

Wind power verses wind speed appearances of wind power system is given below in fig. (3.3)

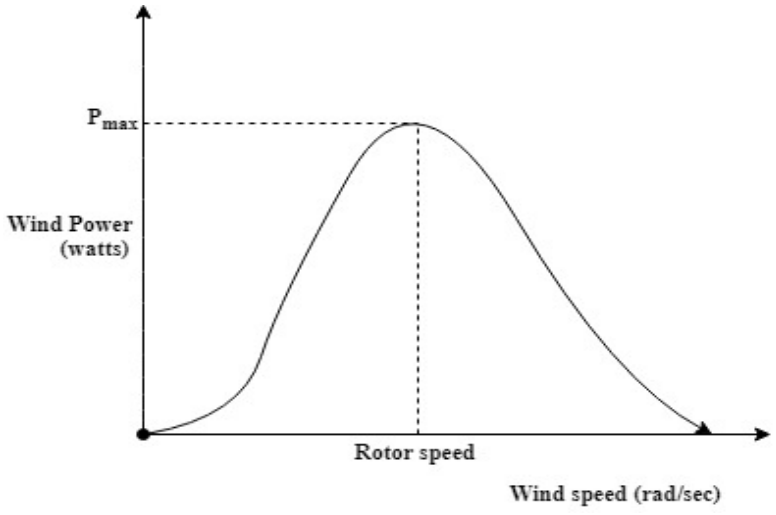


Fig. 3.3 Power vs. speed appearances of wind turbine

At the maximum power point,

$$\frac{dp}{d\Omega} = 0 \tag{3.5}$$

From the chain rule,

$$\frac{dP}{d\Omega} = \frac{dP}{dD} \times \frac{dD}{dV_W} \times \frac{dV_W}{d\Omega_e} \times \frac{d\Omega_e}{d\Omega} \tag{3.6}$$

where,

*P*- Power of wind

Ω - Speed of rotor

$\Omega_e$ - Angular speed of generator-phase voltage

$V_W$ - output voltage of rectifier

*D* – converter duty cycle

For the buck-boost converter equation (3.7) is given as

$$V_0 = \frac{D}{1-D} V_W \tag{3.7}$$

where,

$V_0$ –buck-boost converter output

$V_W$ –buck-boost converter input

From equation (3.7), we can write

$$\frac{dD}{dV_W} = -\frac{D^2}{V_0} \neq 0 \tag{3.8}$$

As a result from the equation (3.8) that $\frac{dD}{dV_W}$ having non-zero and negative value.

The speed of rotor of wind turbine can be associated with the angular speed of generator- phase voltage is given in equation (3.9) as follows:

$$\Omega_e = p.\Omega \tag{3.9}$$

$$\frac{d\Omega_e}{d\Omega} = p > 0 \tag{3.10}$$

where,

*P* – generator pole pairs number

As the equation (3.10) we can conclude that $\frac{d\Omega_e}{d\Omega}$ is non–zero and positive value.

The rectifier output voltage which is proportionate to the generator output voltage as in equation (3.11) can be given as

$$V_{ph} = 4.44.f.\varphi.t \tag{3.11}$$

where $f$ is directly proportional to $\Omega_e$

So

$\frac{dV_{ph}}{d\Omega_e} > 0$ $V_{ph}$ is directly relative to $V_W$

$$\frac{dV_{ph}}{d\Omega_e} \approx \frac{dV_W}{d\Omega_e} > 0 \tag{3.12}$$

where,

$V_{ph}$ - output of generator

$f$ – rotor frequency

$t$ - Number of turns

$\varphi$ - Flux

From equations (3.10), (3.11), (3.12) we see that $\frac{dD}{dV_W}$ , $\frac{d\Omega_e}{d\Omega}$ and $\frac{dV_W}{d\Omega_e}$ having value which is non-zero. Moreover, $\frac{dp}{d\Omega} = 0$ can be possible if and only if $\frac{dp}{dD}$ is zero. As the above equations we are in conclusion that the operational point at which the crest power forced is outlined by changeable the converter duty-cycle [26].

# CHAPTER 4
# ENERGY STORAGE SYSTEM OF A BATTERY

Current study by Grand View Research Inc, meanwhile, demonstrates that the market growth of battery energy storage system for these anticipated to boost further over the next decade, and with increasing battery usage, demand for more sophisticated battery storage over this era will be fuelled.

The adaptation of Alternating Current (AC) to Direct Current (DC) is carried out through the Energy Storage System of a Battery, it has the control scheme and batteries of electronic devices. Battery operation here is the adaptation of electrical energy for storage purposes into the chemical energy. Batteries are discharged and charged using the DC power.

Bi-directional electronic devices regulate the flow of electricity between batteries and energy systems. However the different advantages and disadvantages, energy capacity, weight, size, cost power are based on the type of battery. Lead-Acid, Lithium Ion, Nickel Cadmium, Nickel Metal Hydride are significant types of technologies for storage of energy.

Long cycle life, from top to toe energy density, high sodium sulphur battery charging or discharge efficiency is high. Batteries like Nickel Cadmium (Ni-Cd) are of better quality comparing to the batteries like Lead-Acid [27,28] and requires low maintenance. Compared to the Lead-Acid battery moreover the cost of these batteries is more. It's a costly alternative option.

## 4.1 Overview of Battery Energy Storage System

Lithium-Ion batteries are the maximum energy density among entirely battery types. Usually they are currently being used in computers, cell phones, etc. and this technology is being developed in dispersed applications for energy storage. However due to high costs and partial technology bids. It commands the electronics market because of its availability in various sizes: slight, average and significant renewable energy systems and larger rate of development growth.

Changes in the wind and solar PV generation outputs [29,30] will change in BESS output during coupled operation, and BESS must be counterbalance through rapid variations in output power. For an associated coupled system, the rate dissimilarity control or ramp rate controller is applied to level their power oscillations. This information is managed by the Battery Energy System regulator and evaluations each battery cell's state of charge (SOC) and

capacity and protects all cells operating within the considered SOC range. The economic in addition with the technical merits of energy storing systems are as follows on a lesser scale:

- Improving the quality of electrical supply and reliability.
- It provides backup power for critical loads.

By electricity in the future, that is anticipated that the much more applications will be powered by electricity produced from renewable sources as opposed to combustion motors and energy generation from the other renewable resources, and because of these renewables will absorb as an intermediate storage system, BESS advances are anticipated to contribute to the fast implementation in future.

### 4.2 Advancement for renewable energy applications

Due to changing of the weather upon which renewable energy sources has mostly depend, the need is to balance energy demand from renewable energy supply through reliable energy storage systems (ESS) becomes essential. The common categories of the ESS technologies in recent time include the mechanical, electrical and electrochemical (or battery) energy storage systems.

While most of technologies are not commercially viable at present due to some of their limitations, the battery energy storage system (BESS) are having the incremental market entries and continual improvements for use in different renewable energy applications in transportation, energy back-up, smart grid systems etc.

The battery energy storage system (BESS) has witness the incremental market growth in recent years due their continual improvements which have also contributed to the extension of their applications range. In comparison with the other energy storage system (ESS) technologies in this review, the BESS has more tenacity to contribute to a faster electric future due to their simple-efficient way of storing energy and their less complexity in interfacing with common renewable energy sources in the recent time, mostly solar and wind energy.

In the recent time, modern battery technologies such as Lithium, Sodium-Sulphur and Flow batteries having more usage in electric applications when compared with other ESS technologies. It can be expected as the increasing demands and advancements of BESS continue, battery technology may not be obsolete in near future, rather more improved battery technology with more durability, increased energy density and higher efficiency all at a reasonable costs may soon be realized, thus contributing to a faster realization of electric future

# CHAPTER 5

# MPPT ALGORITHIM

## 5.1 INCREMENTAL CONDUCTANCE MPPT TECHNIQUE

The main shortcoming of the *perturb and observe* technique is the regulator fine-tunes the voltage by a slight amount from array and measures the power, if the power upsurges, further alterations in that course are annoyed until the power no longer intensifications which is stated as the perturb and observe method in addition is the usually, though this method can results in the oscillations of output power. [31] It is mentioned to as a *hill climbing* method, since it be subject to on increase of the power curve against voltage below the maximum power point, and the fall directly above that point. [32] Perturb and observe is furthermost commonly used MPPT technique due to its effortlessness of enactment. [33] Perturb and observe technique may result in top-level competence, provided that a proper analytical besides adaptive hill climbing approach has implemented[34] and to track the peak power below the fast changing atmospheric condition is overwhelmed by the incremental conductance method .

## 5.2 Comparison of algorithms

Individually the incremental conductance and perturb and observe are illustrations of "hill climbing" approaches that be able to find the local extreme of the power curve for the functioning condition of the PV array, and deliver maximum power point .

The perturb and observe technique involves the oscillating output power around maximum power point even though under steady state irradiance.

The incremental conductance scheme has benefit against the perturb and observe (P&O) technique that it can regulates the maximum power point deprived of oscillating around the maximum value [32]. It can accomplish the maximum power point tracking further down hastily changing irradiation conditions with advanced accurateness than perturb and observation technique. Moreover, the incremental conductance technique can produce the fluctuations (inadvertently) and can perform unpredictably under numerous swiftly altering of the atmospheric circumstances. The sampling frequency is to reduced due to higher complication of the algorithm as compared to P&O scheme [32].

In the continuous voltage ratio (or "open voltage") technique, the current from the photovoltaic array essential be set to zero transitorily to measure the open circuit voltages and then subsequently set to a predetermined percentage of voltage measured, usually around 75% [36].

Energy may be unused during the time the current is usual to zero. The approximation of 75% as MPP voltage ratio is not essentially to be precise. Although the simple and low-cost to contrivance, the disruptions reduce the array proficiency and do not confirm to finding actual maximum power point. Moreover, efficiencies of systems influence above the 96% [23].

### 5.3 Modelling of IC MPPT technique

The incremental conductance can regulate that MPPT has touched Maximum power point and stop perturbing the operational point. If this condition is not satisfies, the direction in which MPPT operating point would be perturbed can be considered using the relationship between $\frac{dI}{dV}$ and $-\frac{I}{V}$. The relationship is derived from the element that the $\frac{dP}{dV}$ is negative value when the MPPT is to right side of the MPP and positive value when it is left side of MPP. This procedure has a the benefit over the Perturb & Observation that it can regulate when MPPT has touched the MPP, where P&O oscillates within the MPP. Moreover, the incremental conductance track efficiently increasing and decreasing according to the irradiance conditions with greater accuracy than P and O.

Fig 5.1 illustrate that the slope of the P-V array curve of power curve has zero value at the MPP increasing on the left side of the MPP and reducing on the right side of the MPP. The general equations for this technique are as given in equation (5.1). (5.2) and (5.3)

$$\frac{dI}{dV} = -\frac{I}{V} \quad is\ at\ MPP \tag{5.1}$$

$$\frac{dI}{dV} > -\frac{I}{V} \quad is\ left\ of\ the\ MPP \tag{5.2}$$

$$\frac{dI}{dV} < -\frac{I}{V} \quad is\ right\ side\ of\ the\ MPP \tag{5.3}$$

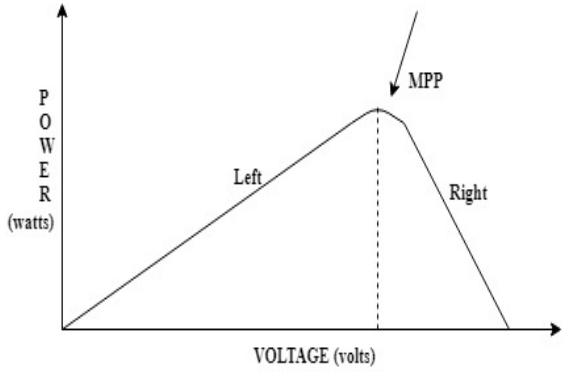


Fig. 5.1. MPPT characteristics of PV

### 5.4 Incremental conductance approach of MPPT algorithm

In this method of incremental conductance method deeds the postulation of the ratio of change in conductance output is equal to the negative conductance output of instantaneous conductance. From the power equation 5.4.,

$$P = VI \tag{5.4}$$

$$\frac{\partial P}{\partial V} = \frac{[\partial (VI)]}{\partial V} \tag{5.5}$$

MPP as $\frac{\partial P}{\partial V} = 0$

The above shown in equation (5.5) can be written in relations of voltage of array and current of array as

$$\frac{\partial I}{\partial V} = - \frac{I}{V} \tag{5.6}$$

However, MPPT normalizes the PWM control DC-DC boost converter signal when this condition $\left(\frac{\partial I}{\partial V}\right) + \left(\frac{I}{V}\right) = 0$ is satisfy. In this scheme of incremental conductance peak power of segment lies at the above 97% of the incremental conductance. In conclusion flow chart of the incremental conductance MPPT is given below in fig 5.2. [31]

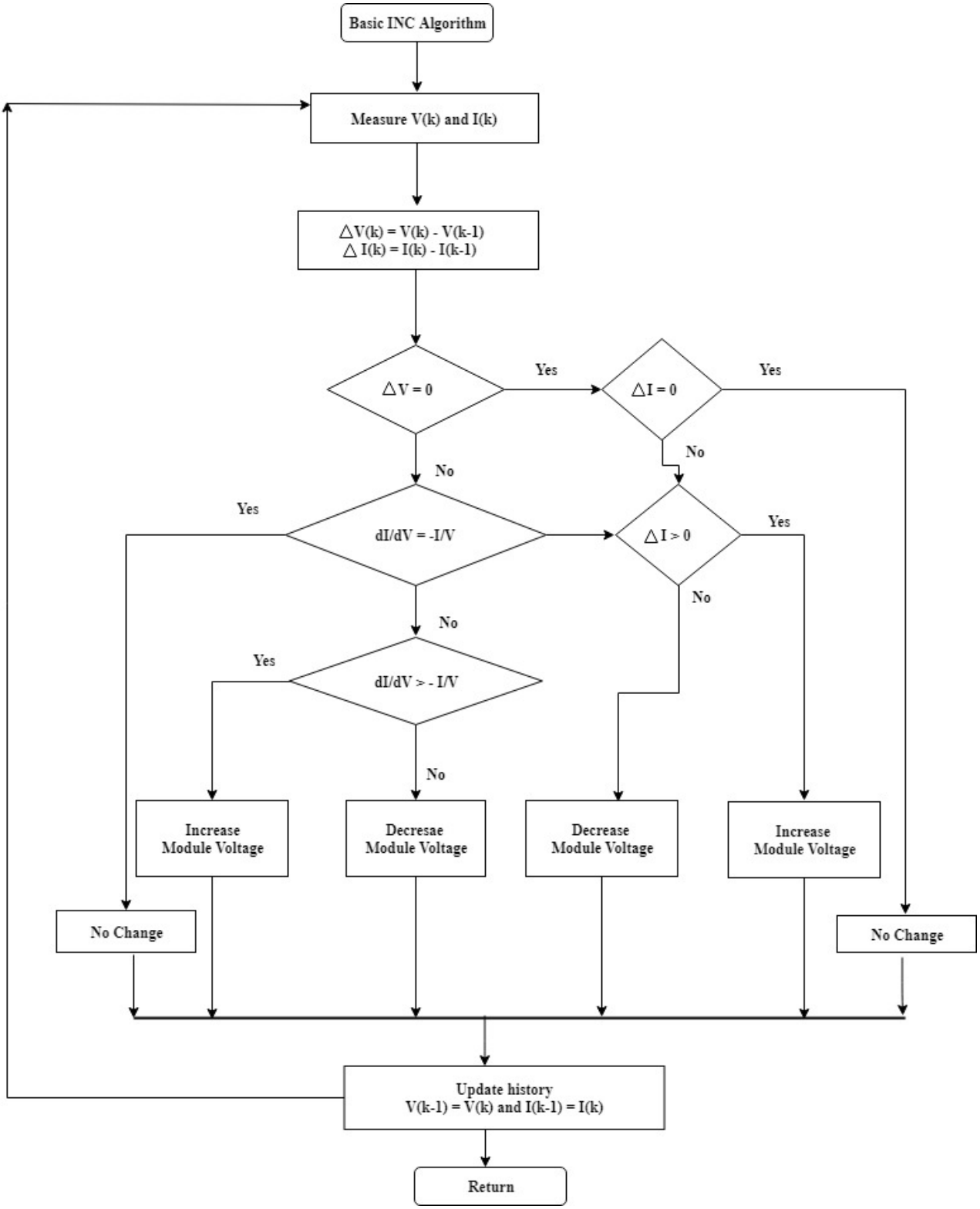


Fig. 5.2. Incremental conductance MPPT flow chart [31].

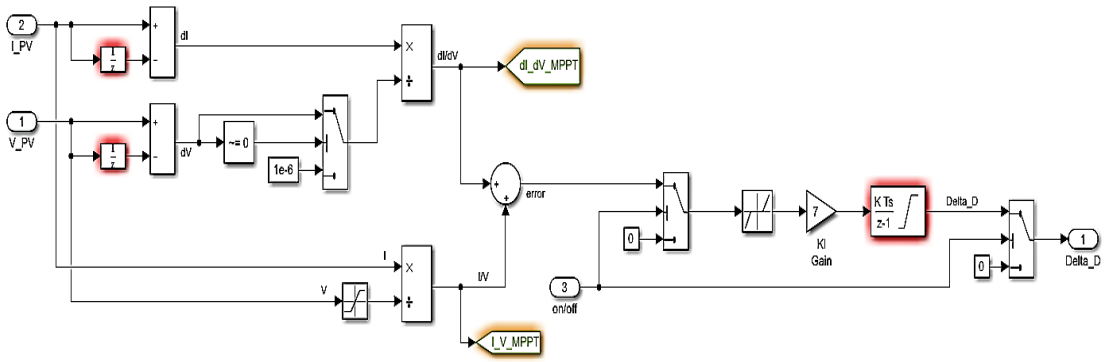


Fig. 5.3. Simulink setup for the Incremental Conductance Method.

Above fig. 5.3 illustrate the simulation setup for incremental conductance algorithm through which maximum power point would be tracked for hybrid (PV-Wind) system.

# CHAPTER 6

# RESULT AND DISCUSSION: CASE STUDY

The whole system designed of the Hybrid (PV-Wind) system is simulated by means of SIMULINK. A 20-kW wind, 4.5-kW of PV and 12 Volts, 24 Ah Battery Energy Storage System hybrid system has been considered. Moreover, system supplies power to a mostly resistive load and RLC load with 495 W, 200Var inductive and 600 Var capacitive.

The simulation study of system constraints are listed below in addition to envisage the actual features the three energy bases are modelled precisely in a SIMULINK.

The simulation is done in the two parts. (1) PV and Wind as separate source of generation fulfilling the load demands. (2) Hybridization of the (PV-Wind) as a source.

The results are attained at variable radiation and variable wind speed for 5 days. First wind turbine is experienced with the constant mechanical load and different results are obtained of power output with different speed of wind of the wind turbine.

The simulation time is for 24 hours and taken as 2.4 seconds.

Here, for simulation we are considering two cases. Simulation has done with wind speed constant and solar radiation constant and temperature in addition to with wind speed constant and variable levels of radiation.

Fig. 6.1 illustrate the constructional diagram of the hybrid system for a Simulink setup.

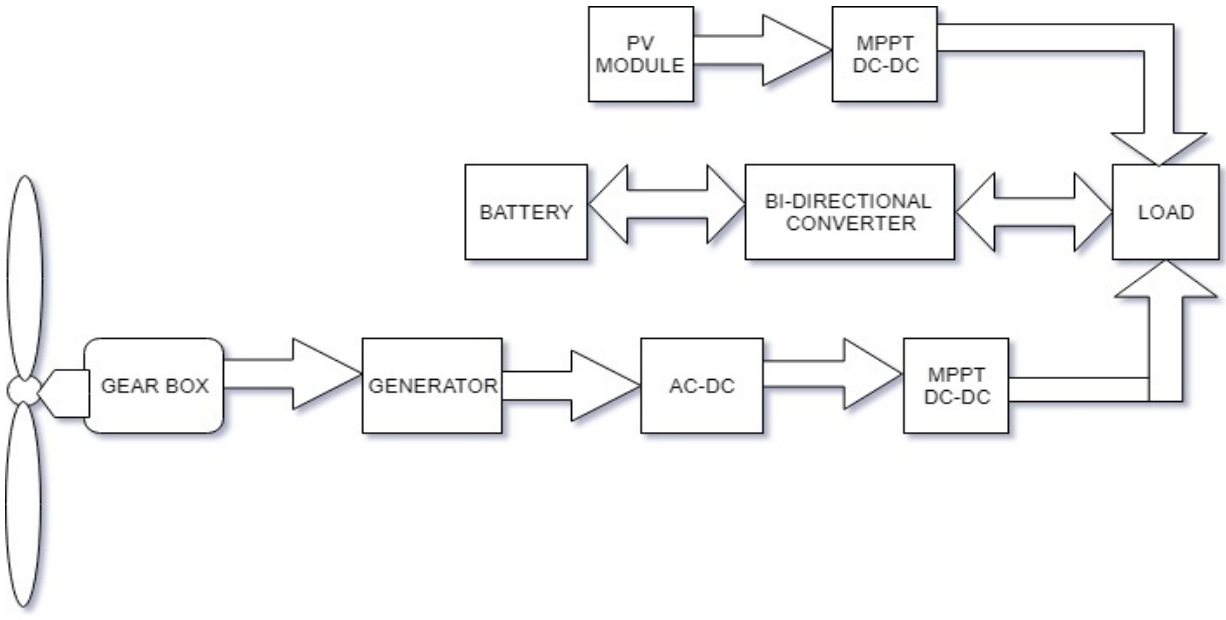


Fig. 6.1 Simulink setup for Hybrid system.

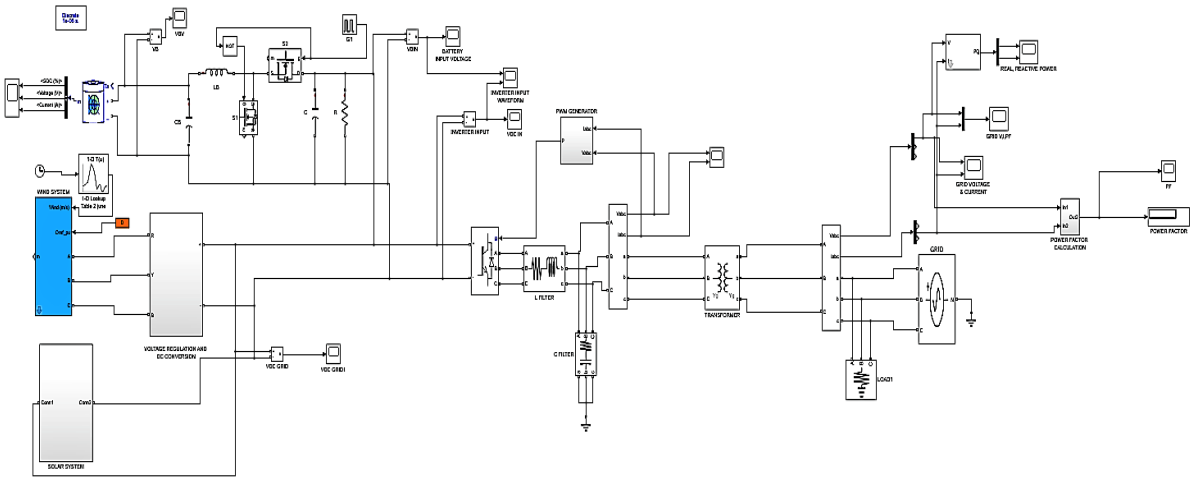

Fig. 6.2 Hybrid Wind-PV System simulation diagram

Above fig. 6.2 is the diagram for the hybrid (PV-Wind) system simulation.

### *6.1 Case I : With wind speed of 15 m/s for wind system and radiation, temperature at STC for PV module at the constant value*

In this case simulation is done with constant wind speed which is of rated wind speed of wind turbine 15 m/s) and PV panel radiation of (1000 W/m$^2$ and 25$^0$ C). The DC power shared by Wind Energy power system is of 15 kW and PV of 5 kW.

Fig. 6.3. shows the battery voltage at constant wind speed and temperature.

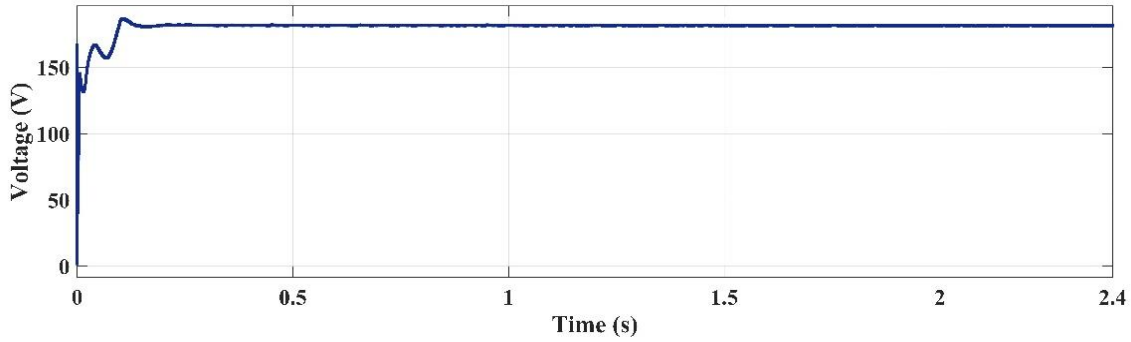


Fig. 6.3 Battery voltage at constant value.

Fig. 6.4. shows the battery current at constant wind speed and temperature.

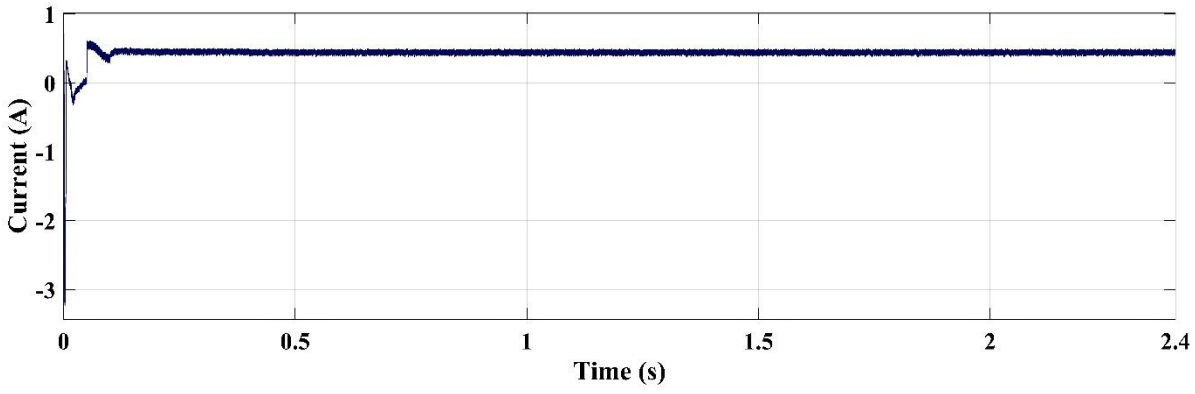


Fig. 6.4 Battery current at constant value

Fig. 6.5. shows the SOC of while charging of a battery energy storage system.

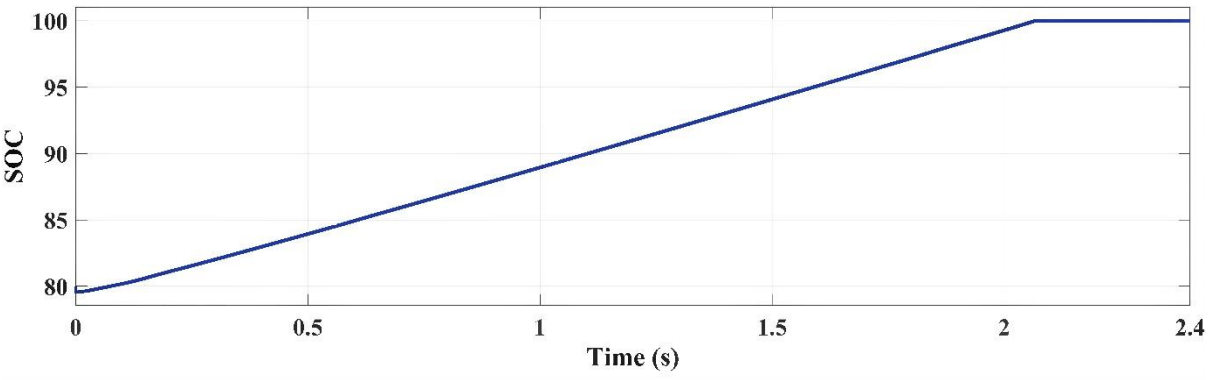


Fig. 6.5 Charging of battery

we can observe from the above figure that during charging state of charge (SOC) of the battery has slowly rising and likewise during charging current seen be negative. From this observation can made at 78% SOC battery voltage is seen to be 186 volts from this we are in conclusion as state of charge of battery is increased which tends to exceeds the battery voltage to its nominal voltage.

Fig. 6.6 shows the battery discharging, from here battery starts providing voltage which is constant and state of charge tends to reducing and the battery voltage would be seen as a constant in fig. 6.7.

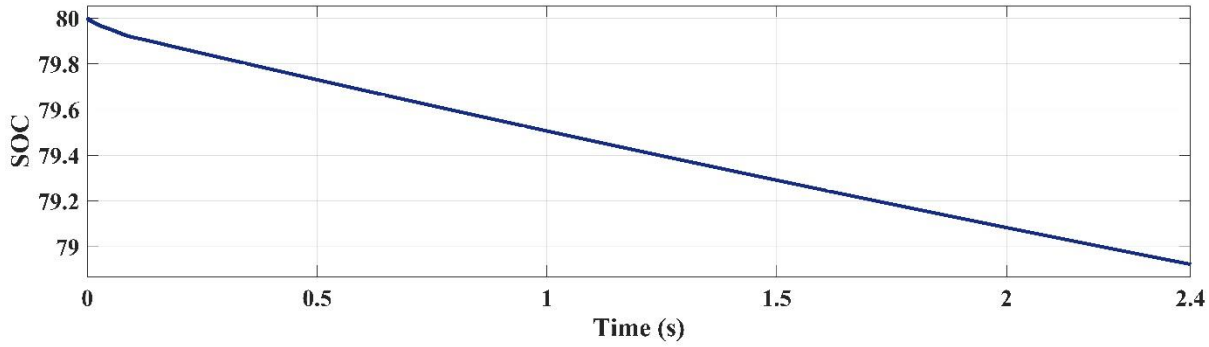


Fig. 6.6. Discharging of battery

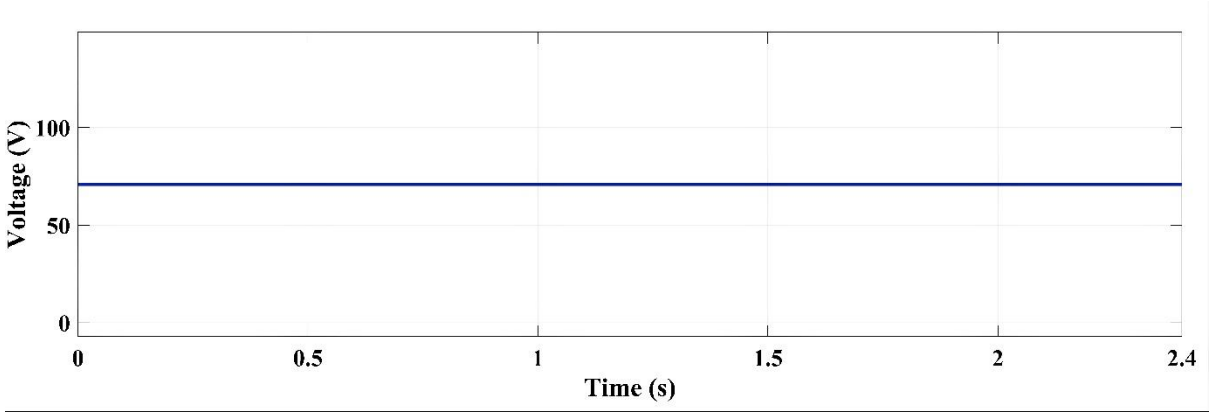


Fig. 6.7 DC Voltage at constant wind speed and temperature.

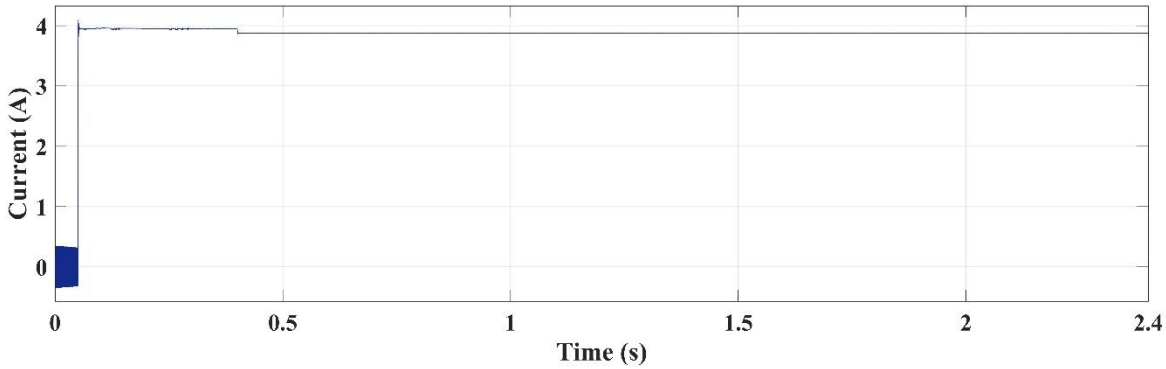


Fig. 6.8 Load Current at constant wind speed and temperature.

we can see from the above figures 6.6. that throughout discharging, battery starts delivering voltage constant and state of charge start reducing in addition to discharging current becomes positive, which demonstrate battery is delivering the power to the load shown in fig. 6.8.

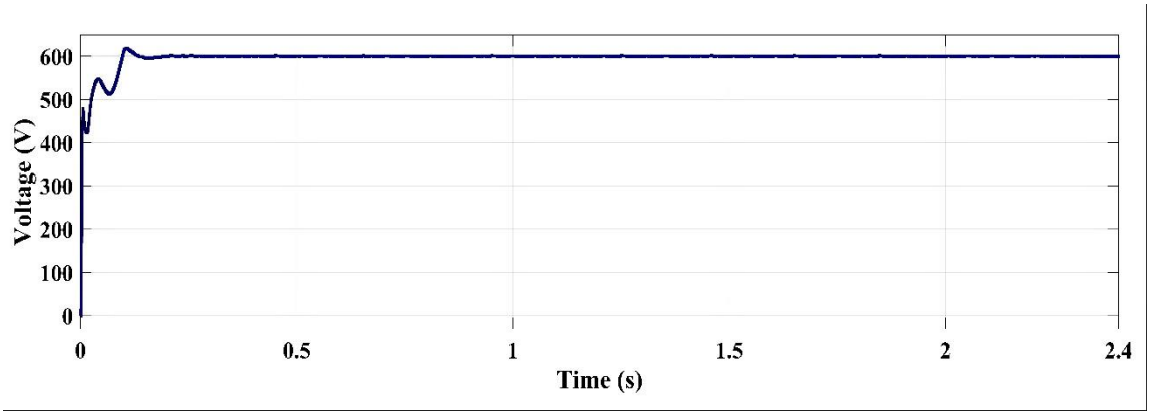


Fig. 6.9. Load Voltage for combined system at MPP

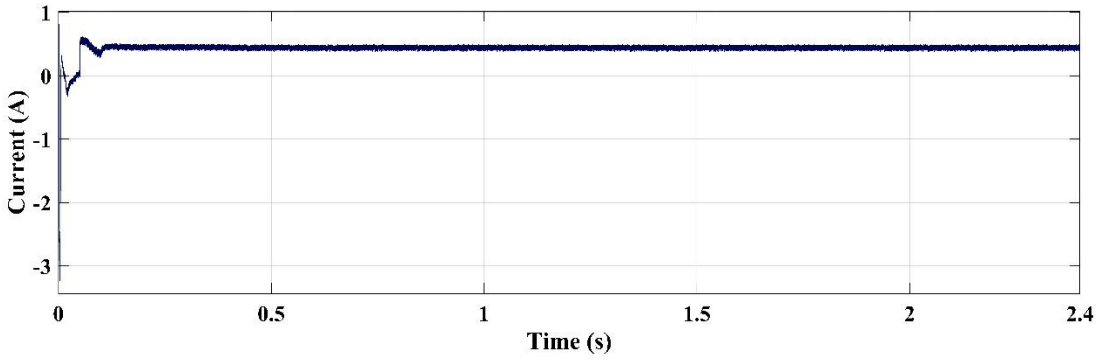


Fig. 6.10. Load Current for combined system at MPP

The operation point of the system (PV, Wind and BESS) output is drawn by maximum power point tracing system which is shown in the fig 6.9, load voltage and current of the combined system at which maximum power is attained as shown in the above figure 6.9 and 6.10. Here maximum voltage traced is 649 volts.

### *6.2 Case II : With variable radiation, variable wind speed and temperature at STC for PV module for the 5 days data*

This case is simulated with different wind speed for which the wind turbine and different radiation of PV module. The practical agitate data is listed in table 6.1. taken from the weather data from 1 JUNE 2019 to 5 JUNE 2019 of 24 hours.

| | 01-Jun-19 | | 02-Jun-19 | | 03-Jun-19 | | 04-Jun-19 | | 05-Jun-19 | |
|---|---|---|---|---|---|---|---|---|---|---|
| Hour | Temp. ℃ | Wind Speed m/s | Temp. ℃ | Wind Speed m/s | Temp. ℃ | Wind Speed m/s | Temp. ℃ | Wind Speed m/s | Temp. ℃ | Wind Speed m/s |
| 00:00 | 35.58 | 1.61 | 32.59 | 3.31 | 31.99 | 3.22 | 33.53 | 4.59 | 33.85 | 2.7 |
| 01:00 | 33.39 | 2.12 | 31.14 | 3.41 | 30.54 | 3.31 | 32.39 | 4.24 | 32.34 | 2.84 |
| 02:00 | 30.9 | 2.45 | 29.95 | 3.51 | 29.53 | 3.71 | 31.26 | 4.05 | 30.64 | 3.01 |
| 03:00 | 29.21 | 2.9 | 29.17 | 3.9 | 29.08 | 4.28 | 30.32 | 4.11 | 29.31 | 3.21 |
| 04:00 | 27.4 | 3.52 | 28.68 | 4.22 | 28.57 | 4.81 | 29.64 | 4.43 | 28.31 | 3.35 |
| 05:00 | 26.31 | 4.39 | 28.19 | 4.54 | 28.11 | 5.06 | 29.05 | 4.74 | 27.54 | 3.44 |
| 06:00 | 29.44 | 5.44 | 31.5 | 5.86 | 31.09 | 7.42 | 31.35 | 5.41 | 30.89 | 3.11 |
| 07:00 | 32.8 | 7.49 | 34.07 | 8.14 | 33.97 | 9.35 | 34.18 | 6.14 | 35.04 | 4.63 |
| 08:00 | 36.23 | 8.47 | 36.24 | 9.71 | 35.66 | 9.52 | 36.62 | 6.58 | 38 | 4.81 |
| 09:00 | 38.8 | 8.42 | 38.61 | 9.3 | 37.39 | 8.99 | 38.67 | 6.58 | 40.25 | 5.11 |
| 10:00 | 41.09 | 7.68 | 40.72 | 8.67 | 39.63 | 8.28 | 40.51 | 6.19 | 42.53 | 4.69 |
| 11:00 | 43.21 | 6.3 | 42.56 | 7.52 | 41.53 | 7.37 | 42.15 | 5.48 | 43.86 | 3.26 |
| 12:00 | 45.14 | 4.25 | 44.1 | 5.87 | 43.31 | 5.91 | 43.55 | 4.44 | 45.15 | 1.6 |
| 13:00 | 46.28 | 1.64 | 45.09 | 3.65 | 44.37 | 4.43 | 44.67 | 3.14 | 45.95 | 2.7 |
| 14:00 | 46.96 | 2.94 | 45.73 | 2.26 | 45.24 | 1.9 | 45.59 | 1.86 | 46.36 | 3 |
| 15:00 | 47.06 | 3.52 | 46.08 | 3.23 | 45.51 | 1.1 | 44.47 | 3.42 | 46.46 | 3.3 |
| 16:00 | 46.83 | 3.61 | 45.93 | 3.71 | 45.43 | 1.81 | 45.02 | 4.04 | 46.12 | 3.32 |
| 17:00 | 46.24 | 3.54 | 45.41 | 3.72 | 44.96 | 1.48 | 44.49 | 4.12 | 45.61 | 3.34 |
| 18:00 | 44.65 | 3.7 | 44.36 | 1.8 | 43.59 | 3.97 | 42.8 | 3.32 | 44.37 | 1.3 |
| 19:00 | 41.32 | 2.83 | 42.08 | 1.57 | 40.47 | 3 | 39.68 | 2.48 | 42.14 | 1.2 |
| 20:00 | 39.22 | 2.96 | 41.3 | 1.7 | 38.59 | 3.92 | 37.83 | 3.16 | 40.98 | 0.86 |
| 21:00 | 37.18 | 3.04 | 39.51 | 2.67 | 36.97 | 4.33 | 36.14 | 2.97 | 39.34 | 1.1 |
| 22:00 | 35.61 | 3.2 | 37.51 | 3.11 | 35.73 | 4.59 | 35.41 | 2.55 | 37.89 | 1.89 |
| 23:00 | 34.05 | 3.31 | 34.21 | 3.21 | 34.62 | 4.78 | 34.89 | 2.42 | 36.48 | 2.27 |

Table 6.1. Hourly weather data of temperature and wind speed.

## 6.3 Simulation results for charging/discharging

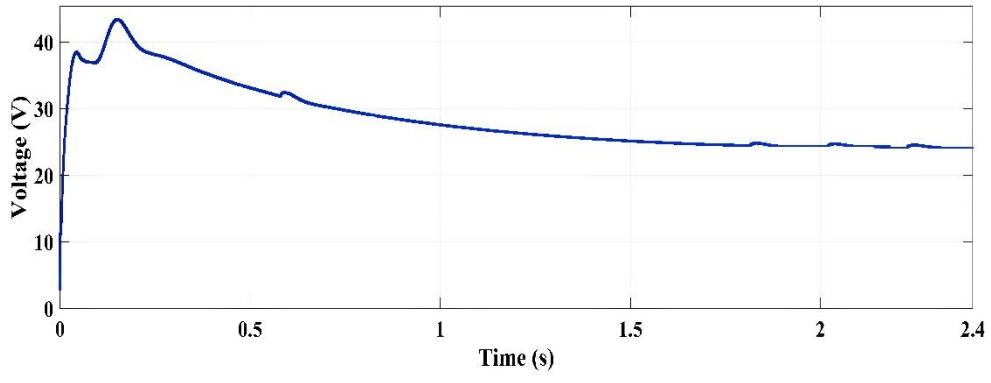


Fig. 6.11. Voltage across the battery.

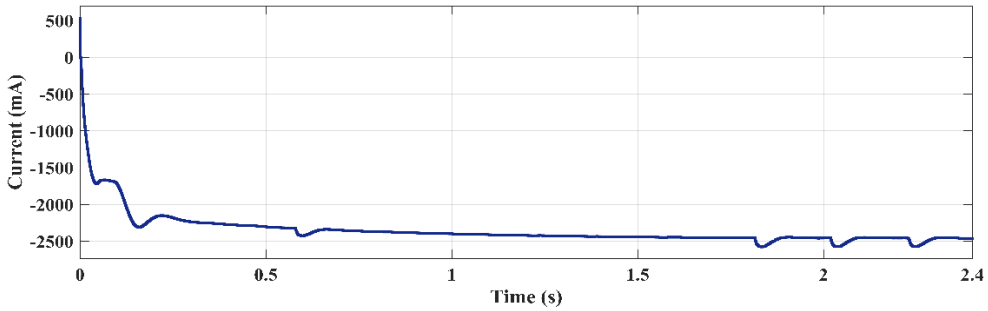


Fig. 6.12. Current through the battery.

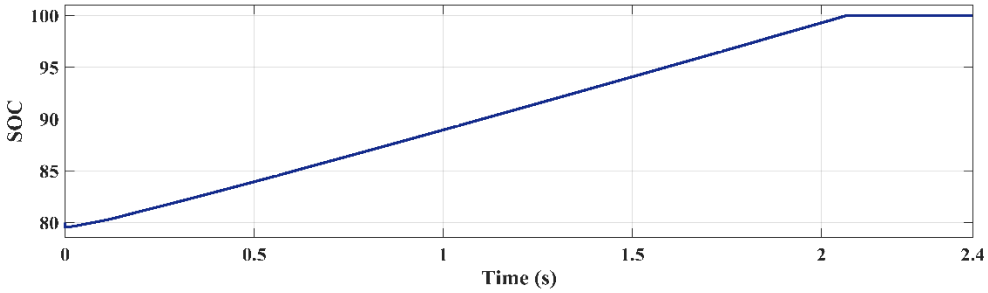


Fig. 6.13. SOC of the battery while charging.

From the above fig 6.11, 6.12, and 6.13 we can detect that during the charging of state of charge (SOC) of battery is slowly rising and also charging current is seen as negative [47]. From that in conclusion is 78.5% SOC voltage of a battery is around 45.44 volts beside state of charge of battery is improved voltage of a battery exceeds to that of nominal voltage. Here the spikes shown in the above figure is due the temperature and wind speed variation. In particular, with the wind speed and temperature reduces the power communal by the mutually, sources declines which consequences into discharging.

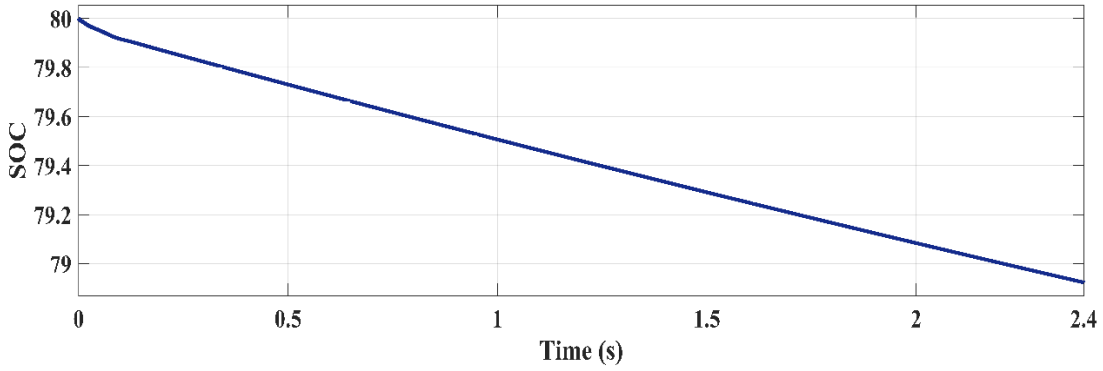


Fig. 6.14. SOC of the battery while discharging.

From figure 6.14 we can understand that during the discharging of the battery it starts supplying voltage which is constant and state of charge starts reducing in addition with the discharging current would be positive, in conclusion with that the battery is providing the power to the load.

## 6.4 OUTPUT AFTER MPPT

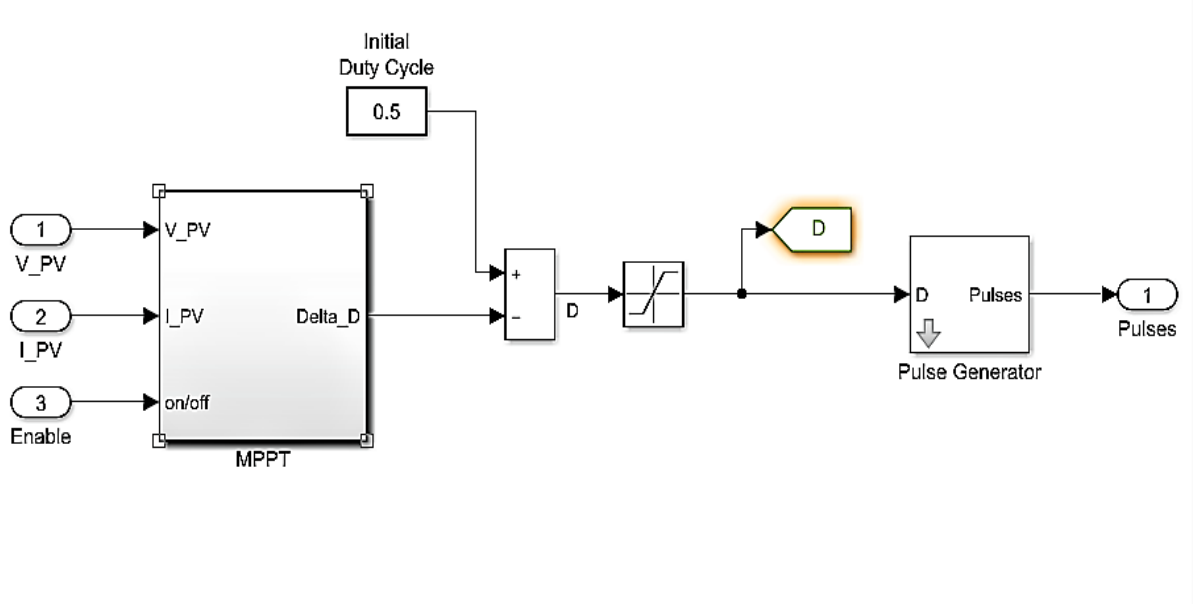


Fig. 6.15. Modelling Stage of MPPT

Fig 6.15 shows the modelling stage of MPPT, here load voltage and load current from the wind, PV and the battery are given as a input and then initialize with a duty cycle of 0.5 proceeding with a pulse generator to apply the algorithm.

Output voltage and power after maximum power point tracing are established in the figure 6.16, respectively. As we observe from the fig 6.16, maximum power attained at voltage 496.68 volts, from fig 6.16 we are in conclusion to track the output voltage where the maximum power achieved is about 496.68 volts.

Figure 6.16 is the load voltage at MPP, from the fig we can see that the transitions during the sunrise and the sunset, and due to the variations in the wind. During the sunrise it rises the peak value and slowly settles down after some time.

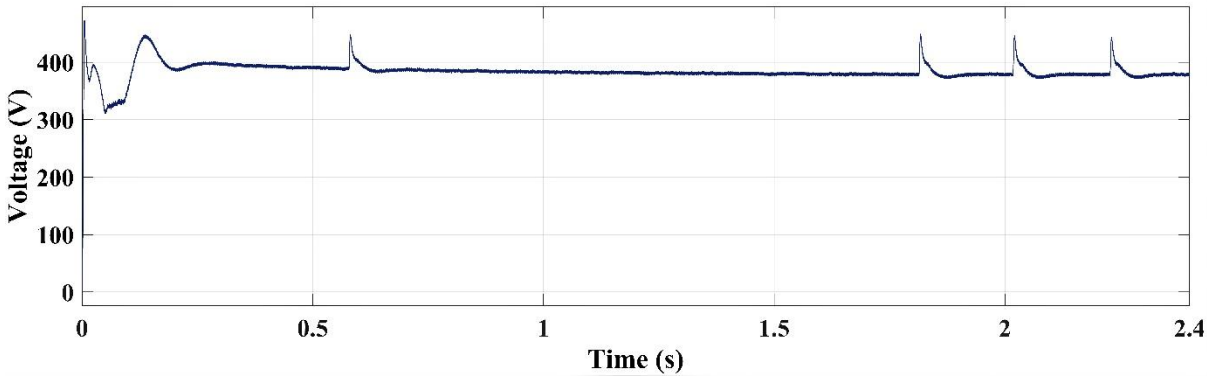


Fig. 6.16. Load Voltage at MPP.

The total demand of the power is contented by the total power generated (PV-Wind) and the mutual power is calculated.

Fig. 6.17. shows the power factor and be seen as 0.98.

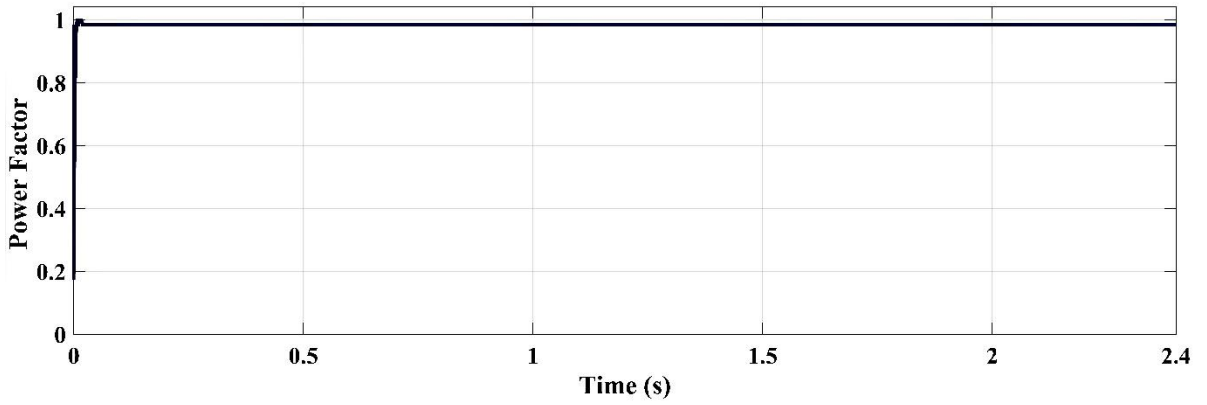


Fig. 6.17. Power factor

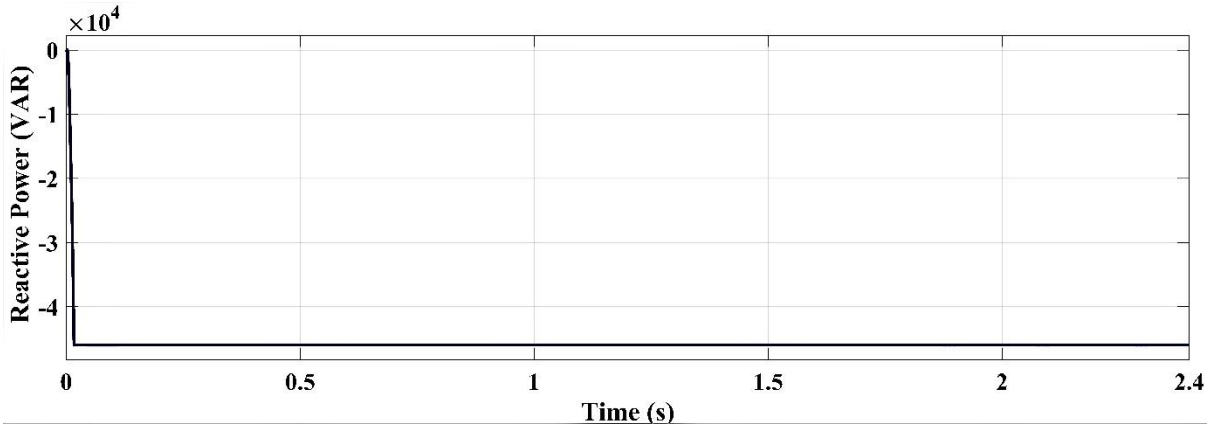


Fig. 6.18. Reactive Power

Above fig. 6.18 shows the reactive power.

(PV-wind) hybrid system have functioned at the same level of voltage and the load voltage remains constant. This is ended by using the PI controller which is associated with (PV-Wind) hybrid and DC-DC converters.

The DC bus voltage, due to the things of the switching of inverter [48] and there are some fluctuations on the dc bus voltage, which is also the voltage input of the inverter.

The output of AC voltage inverter is as shown in fig. 6.19 where the operation of PWM mode, the inverter can be perceived on the voltage output. The output voltage of inverter has functional to load against the transformer voltage can be seen in the fig.6.20 and 6.21 In conclusion to which the three phase line to line voltages have the sinusoidal wave shape having nearly few harmonics. The harmonics cab be reduced by relating with the filter circuits.

The load has chosen to match the generated power of the system. Essentially the voltage at DC load bus and voltage and frequency at AC load bus would be controlled.

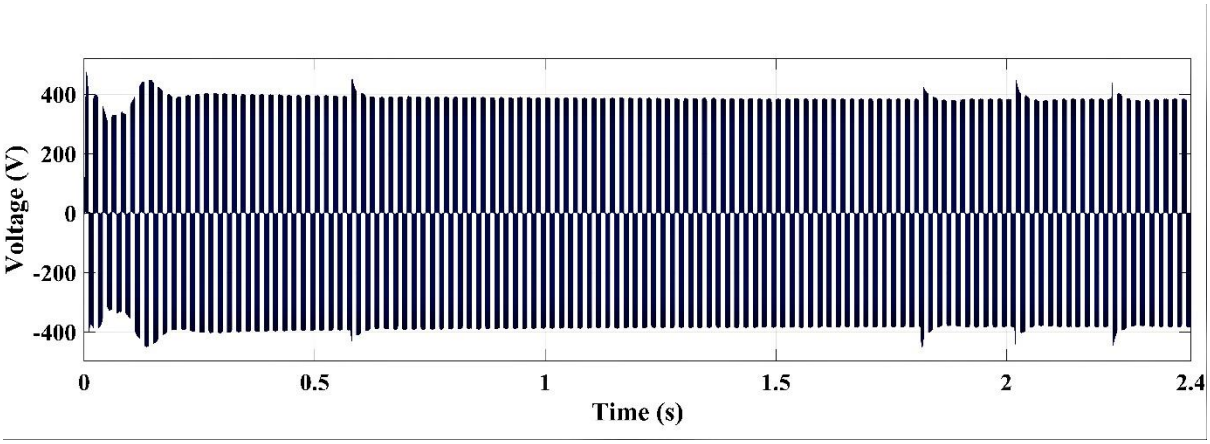


Fig. 6.19. Output AC Voltage of inverter.

The load voltage remain constant and same as the reference value of voltage of 496.68 this value of voltage is taken as the value of reference to operate control approach for the battery. The first control loop has 496.68 V reference value in addition it has to be related with sensed voltage as of DC bus end voltage.

Simulation starts and load begins to flow through current from the system, voltage and current start affecting the functioning values, which is shown in the below given figures for voltage and current, respectively.

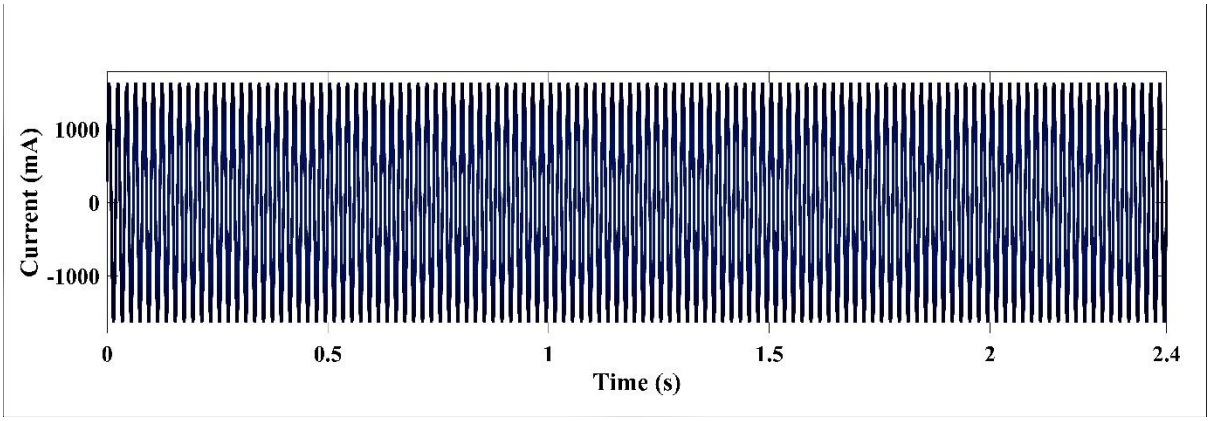


Fig. 6.20. PWM output current.

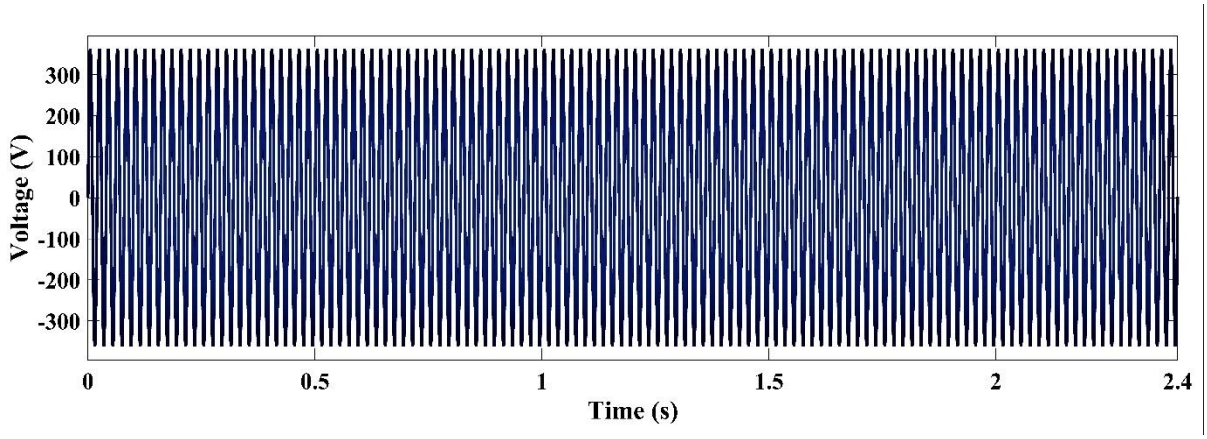


Fig. 6.21. PWM output voltage.

MPPT applied to the Hybrid system ( wind + photovoltaic + BESS) results into efficiency of 97.92%

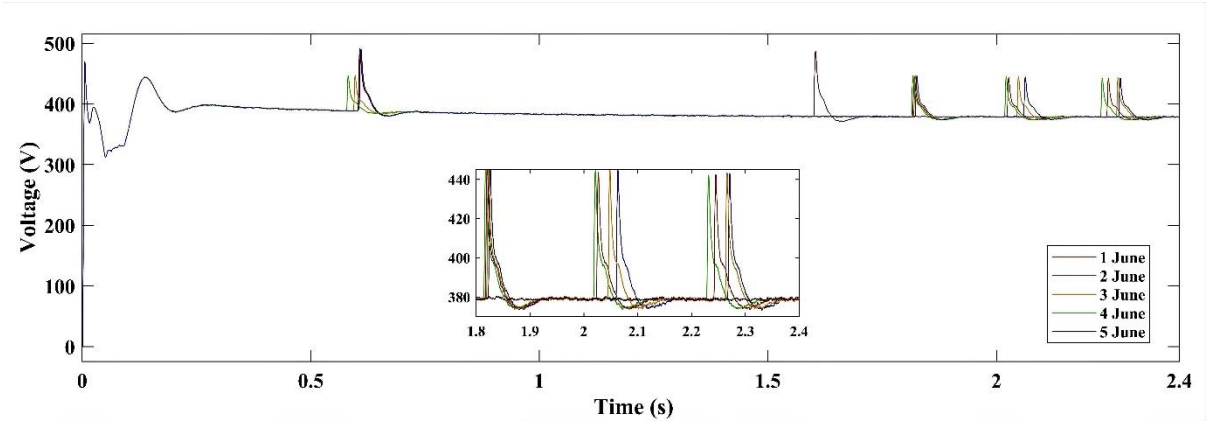


Fig. 6.22 (a) Load Voltage of a combined system for 5 days

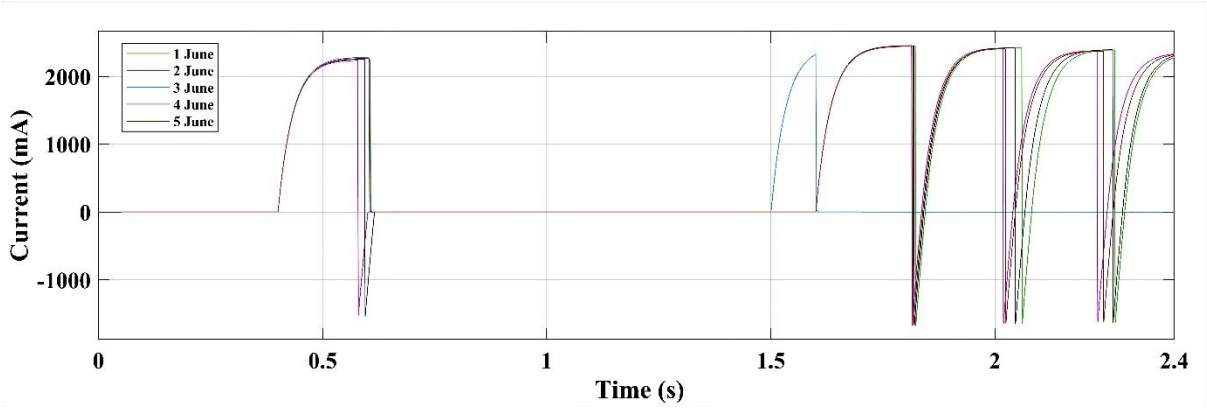


Fig. 6.22 (b) Load current of a combined system for 5 days

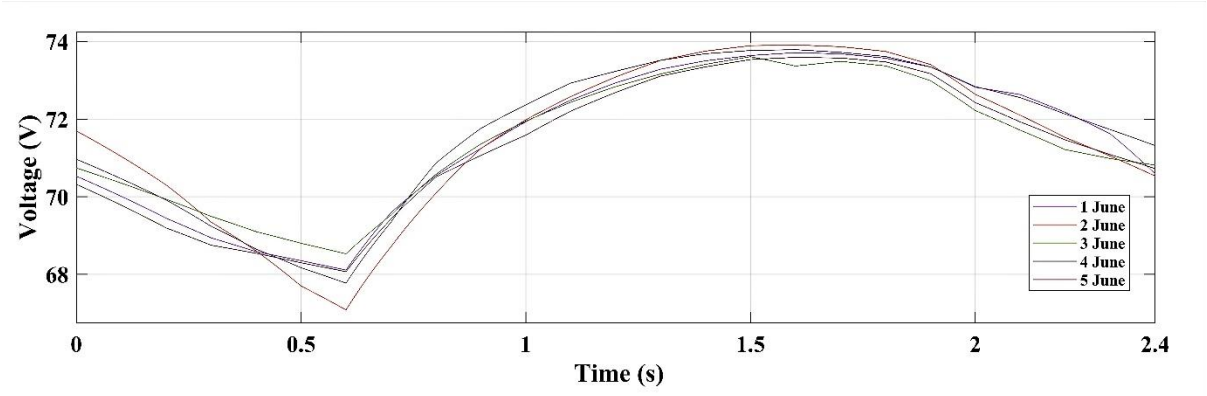


Fig. 6.22 (c) Voltage of PV for 5 days

Fig. 6.22(a) and 6.22(b) shows load voltage and load current for the combined system for 5 days. The transition are seen in the fig 6.22(a) and 6.22(b) are due to the variation in the temperature and wind variation of different days. Higher the temperature or wind variation larger the transition seen. Fig. 6.22(c) is the voltage of a PV system for 5 days with a temperature variation.

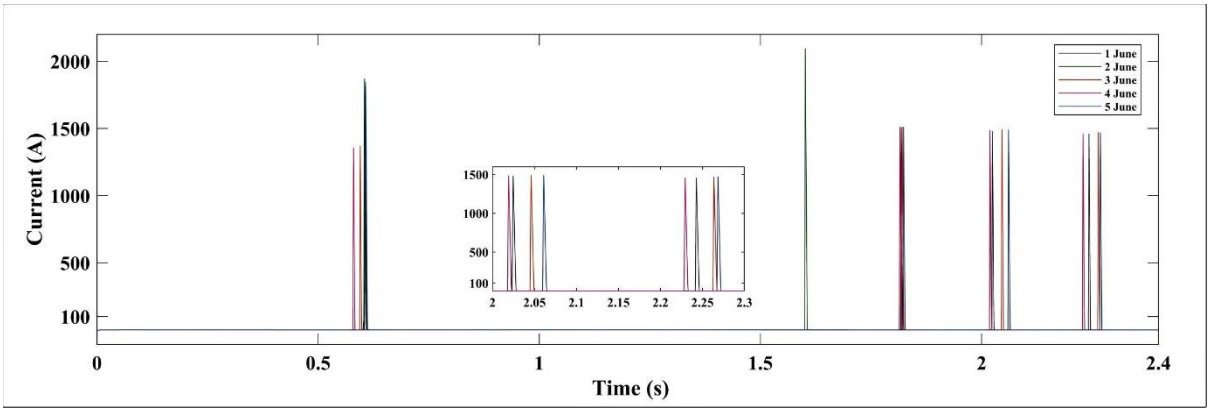


Fig. 6.22 (d) Wind Current for 5 days

Figure 6.23(a) and 6.23(b) stimulate the simulation result of PV system current and voltage from wind system. If the load has changed or applied suddenly to the system then variations happen in the load current of PV as shown in below figure. Variation of the transition also seen in case of the wind voltage with the variation in the wind speed transition are seen in fig. 6.23(b) for the peak there is the maximum wind speed at that particular hour.

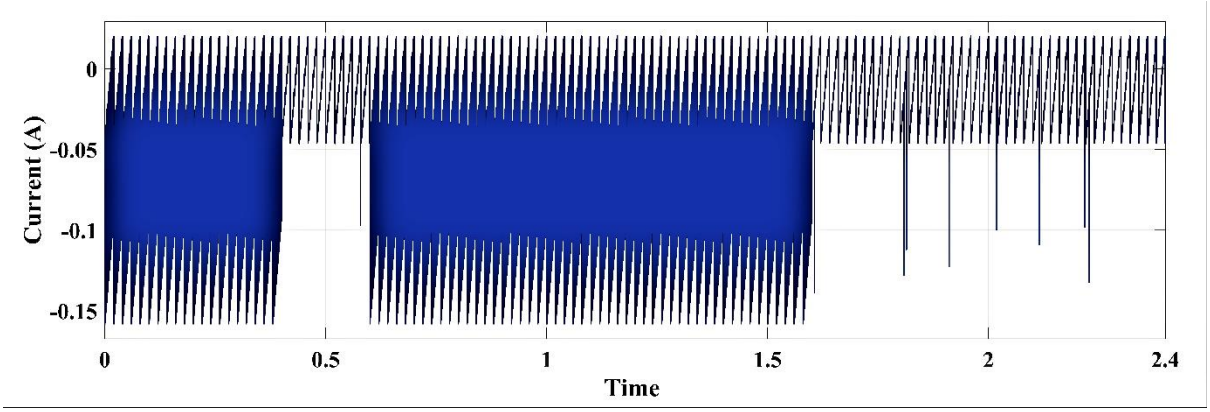


Fig. 6.23 (a) PV system current

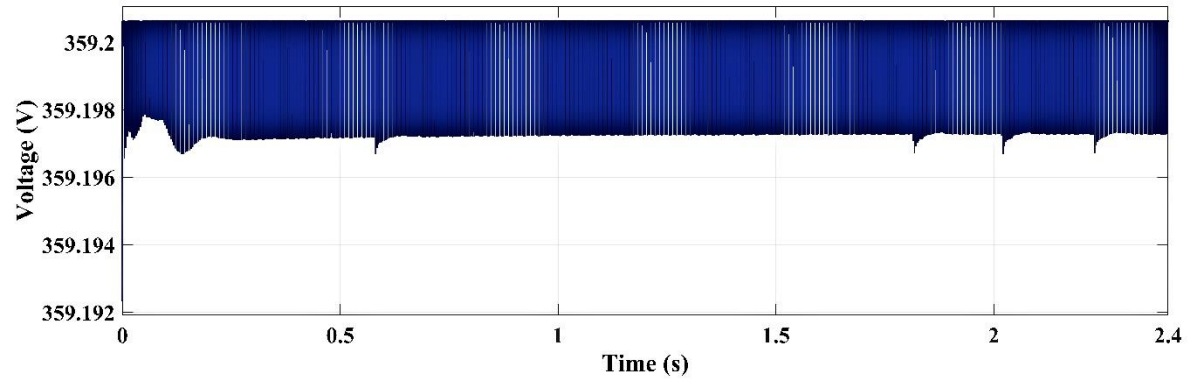


Fig. 6.23 (b) Voltage from wind system.

# CHAPTER 7
# CONCLUSION WITH FUTURE SCOPE

## 7.1. Conclusion

The idea of hybridization of (PV-wind) and battery effectively simulated to encounter the load demand. The efficiency of the incremental conductance MPPT algorithm for overhead hybridization is established. DC link voltage has been maintained and regulated from by means of the DC-DC boost converter and bi-directional DC-DC converter. In conclusion with the simulation we can detect wind and PV mutually have communal 24.5 kW of power that is 89.96% of total power and approximately 10% power has been communal by battery bank.

Under all the functioning conditions to meet the demand of load for the hybrid system (PV, wind and BESS) has measured to give the maximum output power. Battery is supportive to wind or PV system to fulfill the demand of load and also, concurrent and continuous process for load.

The performance of the hybrid system (PV, wind and BESS) increases system dependability and steadiness of supply. So the system could find the place as a eco-friendly, low preservation alternative method to a power. In conclusion from this it becomes a feasible way to yield the electrical energy where the connections of grid are not available particularly in the rural areas.

## 7.2. Future scopes of Research

The scope of work after studying and analyzing the MPPT based Hybrid system is identified as:

- MPP tracked using different procedures and with the combination of algorithms.
- To minimize the transitions occurring during the variation of wind speed and irradiation.
- Battery controller can be designed for more dependable operation and for improved battery life and robustness.
- Modification of algorithm can be tracked with better and improved efficiency.
- With the modified Incremental Conductance (INC) procedure which uses adjustable step size of voltage to estimate the trade-off between the active responses and trade-off among the steady state and dynamic response alternation with admiration to size of the step size.

# REFRENCES


[1] S. Rahman and R. Chedid, "Unit sizing and control of hybrid wind–solar power systems ,"*IEEE Transactions on Energy Conversion*, vol. 12, no.1, pp. 79-85, 1996. T. Markvart "Sizing of hybrid photovoltaic–wind energy systems: solar energy," *IEEE Transactions on Energy Conversion,* vol. 57, no.3, pp. 277-281, 1998.

[2] K. Katti and M.K. Khedkar, "Alternative energy facilities based on site matching and generation unit sizing for remote area power supply," *Renewable Energy,* vol. 32, no.2, pp.1346-1366, 2007.

[3] S.M. Shaahid and M.A. Elhadidy, "Opportunities for utilization of stand-alone hybrid (photovoltaic, diesel and battery) power systems in hot climates," *Renew Energy,* vol. 28, no. 11, pp. 1741-1753, 2003.

[4] E. Koutroulis, D. Kolokotsa, A. Potirakis and K. Kalaitzakis, "Methodology for optimal sizing of stand-alone photovoltaic/wind-generator systems using genetic algorithms," *Solar Energy,* vol. 80, no. 3, pp. 1072-1088, 2006.

[5] A.H. Shahirinial, S.M. Tafreshi, A. Hajizadeh, M. Gastaj and A.R. Moghaddamj, "Optimal sizing of hybrid power system using genetic algorithm," *IEEE Transaction of energy,* vol. 11, no.2, pp. 212-218, 2006.

[6] C. Protogeropoulos, B.J. Brinkworth and R.H. Marshall, "Sizing and techno-economical optimization for hybrid solar photovoltaic/wind power systems with battery storage," *International Journal of Energy,* vol.21, pp. 465-479, 1997.

[7] B. Ai, H. Yang, H. Shen and X. Liao, "Computer-aided design of PV/wind hybrid system," *Renew Energy,* vol.28, no. 10, pp. 1491-1512, 2003.

[8] M.D. Arifujjaman, M. T. Iqbal, E. John , M. Quaicoe and J. Khan, "Modelling and control of a small wind turbine," *IEEE transaction on Energy,* vol.45, no. 4, pp. 778-781, 2005.

[9] B.S. Borowy and Z.M. Salameh, "Dynamic response of a stand-alone wind energy conversation system with battery energy storage to a wind gust," *IEEE Transactions on Energy Conversation,* vol. 12, no. 1, pp. 73-78, 1997.

[10] K. Pavan, A. M. Parimi and K.U. Rao, "Performance Analysis of a two-Diode model of PV cell for PV based generation in MATLAB," *IEEE International Conference on Advanced Communications, Control and Computing Technologies, Ramanathapuram,* vol. 34, no.8, pp. 68-72, 2014.

[11] T. Salmi, M. Bouzguenda and A. Gagtli, "MATLAB/Simulink based modelling of solar photovoltaic cell," *International journal of renewable energy research*, vol.2, no.2, 2012.

[12] S. Meenakshi, K.Rajambal and S. Elangovan, "Intelligent controller for stand-alone hybrid generation system," *IEEE International Conference on Advanced Communications*, vol.4, no.5, pp. 1476-1486, 2006.

[13] N. A. Ahmed and M. Masafumi, "A stand-alone hybrid generation system combining solar photovoltaic and wind turbine with simple maximum power point tracking control," *IEEE Transactions on Energy Conversation, IPEMC* 2, vol.8, no.6, pp. 675-687, 2006.

[14] M. G. Villalva and J. R. Gazoli, "Modelling and circuit based simulation of photovoltaic arrays," *Brazilian power electronics conference (COBEP*), vol.8, no.3, pp. 172, 2009.

[15] G. V. Marcelo and R. G. Jonas, "Comprehensive approach to modelling and simulation of photovoltaic arrays," *IEEE transaction on power electronics*, vol.24, no.5, pp.76-79, 2009.

[16] H. Patel and V. Agarwal, "Matlab based modelling to study the effect of partial shading on PV array characteristics," *IEEE transaction on energy conversion*, vol.23, no.1, pp. 89-91, 2008.

[17] Mohammed and I. Iskender, "Simulation and experimental study of shading effect on series and parallel connected PV modules," *IEEE transaction on energy conversion*, vol.27, no.2, pp. 56-71, 2008.

[18] S. Guo and T. W. Michael, "Analysing partial shading of PV module by circuit modelling," *IEEE transaction on power electronics,* vol. 76, no.2, pp. 798-801, 2011.

[19] X. Zhou, S. Daichun, M. Youjie and C. Deshu, "The simulation and design for MPPT of PV system based on Incremental conductance method," *Wase International conference on information engineering*, vol.34, no.2, pp. 76-79, 2007.

[20] A. Safari and P. Mekhilef, "Simulation and Hardware Implementation of Incremental Conductance MPPT with Direct Control Method Using Cuk Converter *" IEEE transaction on industrial electronics*, vol. 58, no. 4, pp. 67-73, 2011.

[21] S. Rahmani, A. Hamadi and A. Ndtoungou, "Performance evaluation of a PMSG-based variable speed wind generation system using maximum power point tracking," *IEEE electrical power and energy conference,* vol. 67, no. 5, pp. 74-79, 2012.

[22] M. Jamil and R. Gupta, "A review of power converter topology used with PMSG based wind power generation," *IEEE electrical power and energy conference*, vol. 73, no. 6, pp. 81-85, 2012.

[23] E. Koutroulis and K. Kalaitzakis, "Design of a maximum power tracking system for wind-energy conversion application," *IEEE Transaction on industrial electronics*, vol. 53, no. 2, pp. 97-99, 2006.

[24] C. Lin, S. Yang and G.W. Wu, "Study of a non-isolated bidirectional dc-dc converter," *IET power electronics*, vol.6, no. 2, pp. 56-61, 2013.

[25] M. H. Ali, "Wind energy systems solutions for Power Quality and Stabilization," *IET power electronics*, vol.7, no.3, pp. 63-65, 2012.

[26] S. Jalili and R. Effatnejad, "Simultaneous coordinated design of power system stabilizer 3 band and SVC by using hybrid big bang big crunch algorithm in multi-machine power system," *Indian Journal of Science and Technology*, vol. 3, no. 2, pp. 62-71, 2015.

[27] R. Ambika, R. Rajeswari and R. Nivedita, "Comparative analysis of nature inspired algorithms applied to reactive power planning studies," *Indian Journal of Science and Technology*, vol. 4, no. 4, pp. 445-453, 2015.

[28] N. Garimella and N. K. C. Nair, "Assessment of battery energy storage systems for small-scale renewable energy integration," *IEEE Conference on industrial* electronics, vol. 3, no. 8, pp. 1-6, 2009.

[29] D. Sera, T. Kerekes, R. Teodorescu and F. Blaabjerg, "Improved MPPT algorithms for rapidly changing environmental conditions," *IEEE Conference on conversion energy*, vol.5, no. 3, pp. 1614-1619, 2006.

[30] S. Azadeh and S. Mekhilef, "Simulation and Hardware Implementation of Incremental Conductance MPPT With Direct Control Method Using boost Converter," *IEEE Conference on conversion energy*, vol.6, no. 2, pp. 19, 2004.

[31] M. Lokanadham and K.V. Bhaskar," Incremental Conductance Based Maximum Power Point Tracking (MPPT)for Photovoltaic System," *International Journal of Engineering Research and Applications (IJERA)* pp. 56, 2016.

[32] N. Garimella and K. C. Nair, "Assessment of battery energy storage systems for small-scale renewable energy integration" *IEEE Conference on energy conversion*, vol.3, pp. 1-6,2009.

[33] D. Sera, T. Kerekes, R. Teodorescu and Blaabjerg, “Improved MPPT algorithms for rapidly changing environmental conditions,” *IEEE Conference on energy conversion*, vol. 5, no. 2, pp. 1614-1619, 2006.

[34] M. Gheydi, R. Effatnejad and P. Ramezanpour, “Evaluation of uncertainty in hybrid plants, including wind turbine, photovoltaic, fuel cell, and battery system using fuzzy logic,” *Indian Journal of Science and Technology*, vol. 7, no. 2, pp. 113-122,2014.

[35] M. Izadbakhsh, A. Rezvani, M. Gandomkar and S. Mirsaeidi, “Dynamic analysis of PMSG wind turbine under variable wind speeds and load conditions in the grid connected mode,” *Indian Journal of Science and Technology,* vol. 8, no. 14, pp 51864, 2015.

[36] R. Ambika, R. Rajeswari and A. Nivedita, “Comparative analysis of nature inspired algorithms applied to reactive power planning studies” *Indian Journal of Science and Technology*, vol. 8, no. 5, pp. 445-453, 2015.

[37] A. G. Bhave, “Hybrid solar–wind domestic power generating system-case study”. *Renew Energy* , vol. 17. No. 8, pp. 355-358, 1999.

[38] M. D. Arifujjaman, M. T. Iqbal, E. John, M. Quaicoe and K. Jahangir, “Modelling and control of a small wind turbine,” *IEEE transaction on Energy Conversion,* vol.7, pp. 778-781, 2005.

[39] F. Giraud and Z. M. Salameh, “Steady-state performance of a grid-connected rooftop hybrid wind-photovoltaic power system with battery storage,” *IEEE Transactions on Energy Conversion*, vol. 16 no. 1, pp. 1-7, 2001.

[40] C. Meurer, H. Barthels, W. A. Brocke, B. Emonts and H.G. Groehn, “An autonomous supply system with renewable energy,” *Solar Energy*, pp.131-138, 1999.

[41] K.N. Reddy and V. Agarwal, “Utility interactive hybrid distributed generation scheme with compensation feature,” *IEEE Transactions on Energy Conversions*, vol. 22, no. 3, pp. 666-673, 2007.

[42] D. Das, R. Esmaili and N. Dave Nichols, “An optimal design of a grid connected hybrid wind/photovoltaic/fuel cell system for distributed energy production”. *IEEE Transactions on Energy Conversions,* vol. 23, no. 5, pp. 2499-2505, 2005.

[43] J. Huil, A. Bakhshai and P.K. Jain, “A hybrid wind-solar energy system”: A new rectifier stage topology, 25th Annual *IEEE Proceedings of Applied Power Electronics Conference and Exposition (APEC),* pp. 156-161, 2010.

[44] S.K. Kim, J.H. Jeon, C.H. Cho, J.B. Ahn and S.H. Kwon, "Dynamic modelling and control of a grid-connected hybrid generation system with versatile power transfer," *IEEE Transactions on Industrial Electronics*, vol. 55, no. 4, pp. 1677-1688, 2008.

[45] S. Ezhilarasan, P. Palanivel and S. Sambath, "Design and development of energy management system for DG source allocation in a micro grid with energy storage system," *Indian Journal of Science and Technology*, vol. 8, no.13, pp. 58252, 2015.

[46] M. R. Patel, "Wind and solar power systems design analysis and operation," 2nd ed. *Taylor and Francis Group Publishing Co.*, vol. 30, no. 3, pp. 265-266, 2006.

[47] Y. M. Chen, Y.C. Liu , S.C. Hung and C.S. Cheng, "Multi-input inverter for grid-connected hybrid PV/wind power system," *IEEE Transactions on Power Electronics*, vol. 22, no. 3, pp. 1070-1077, 2007.

[48] S. Jain and V. Agarwal, "An integrated hybrid power supply for distributed generation applications fed by nonconventional energy sources," *IEEE Transactions on Energy Conversion* vol. 23, no. 2, pp. 622-631, 2008.